The Wash Igneous Complex of eastern England: A candidate Avalonian source for Sandbian tephra in Baltoscandia and implications for closure of the Tornquist Sea

Tim C. Pharaoh[1,†], Jeremy Rushton[1], Dan Condon[1], Simon Chenery[1], Matt Horstwood[1], Diana Sahy[1], Chris Thomas[2], Elliott Hamilton[1], Charles J.B. Gowing[1], Jonathan Busby[1], Richard Haslam[1], and Trond H. Torsvik[3,4]

[1]*British Geological Survey, Keyworth, Nottingham NG12 5GG, UK*
[2]*British Geological Survey, The Lyell Centre, Research Avenue South, Edinburgh, EH14 4AP, UK*
[3]*Center for Planetary Habitability (PHAB), University of Oslo, 0318 Oslo, Norway*
[4]*School of Geosciences, University of Witwatersrand, Johannesburg 2001, South Africa*

Tim Pharaoh https://orcid.org/0000-0002-0452-5088 tcp@bgs.ac.uk

© 2026 UNITED KINGDOM RESEARCH AND INNOVATION.
GSA Bulletin v.138, p.XX-XX. https://doi.org/10.1130/B38831.1

The Wash Igneous Complex of eastern England: A candidate Avalonian source for Sandbian tephra in Baltoscandia and implications for closure of the Tornquist Sea

Tim C. Pharaoh[1,†], Jeremy Rushton[1], Dan Condon[1], Simon Chenery[1], Matt Horstwood[1], Diana Sahy[1], Chris Thomas[2], Elliott Hamilton[1], Charles J.B. Gowing[1], Jonathan Busby[1], Richard Haslam[1], and Trond H. Torsvik[3,4]

[1]*British Geological Survey, Keyworth, Nottingham NG12 5GG, UK*
[2]*British Geological Survey, The Lyell Centre, Research Avenue South, Edinburgh, EH14 4AP, UK*
[3]*Center for Planetary Habitability (PHAB), University of Oslo, 0318 Oslo, Norway*
[4]*School of Geosciences, University of Witwatersrand, Johannesburg 2001, South Africa*

ABSTRACT

The Wash Igneous Complex (WIC) is a component of a Sandbian (Late Ordovician) calc-alkaline magmatic arc that extends from the Lake District in northern England to the Brabant Massif of Belgium, associated with fast subduction of Tornquist ocean crust separating Avalonia (upper plate) and Baltica (lower plate). Buried beneath the East Midlands and The Wash of eastern England, the WIC is likely to comprise an extensive nested caldera system, underlain by a granite batholith, inferred from geophysical data. New whole-rock geochemical data confirm the calc-alkaline character of the WIC and elucidate relationships with other calc-alkaline magmatic complexes in eastern England. Detailed petrographic and geophysical data indicate that the WIC had the capacity to generate super-eruptions. Evidence for ultraplinian volcanism comes from contemporary, regionally distributed and thick metabentonite tephra in Baltoscandia. New, high-precision U-Pb isotopic (chemical abrasion–isotope dilution–thermal ionization mass spectrometry; CA-ID-TIMS) ages of 454.45 ± 0.13/0.23/0.54 Ma and 454.40 ± 0.11/0.22/0.53 Ma (2σ, Sandbian, Late Ordovician) are reported for zircons from a heterolithic dacitic tuff-breccia and a subvolcanic microgranite respectively, recovered from two deep boreholes that intersect the WIC. These dates are identical, within their analytical uncertainties, with equivalently high-precision U-Pb zircon dates for the Kinnekulle Metabentonite (KKMB; Baltoscandia). A population of younger grains from the breccia yielding a CA-ID-TIMS age of 453.70 ± 0.17/0.26/0.55 Ma (2σ) may correlate with the Lower Grimstorp Metabentonite. The matching U-Pb dates and closely comparable apatite microphenocryst chemistry from WIC rocks and the Baltoscandian tephra suggest the WIC as a primary candidate for much of the composite KKMB.

INTRODUCTION

Plutonic and volcanic rocks of Late Ordovician age are found in northern and eastern England, extending from the English Lake District (Figs. 1 and 2) to The Wash (Pharaoh et al., 1993) with likely correlatives in Belgium (André et al., 1986). These magmatic suites have been attributed to a calc-alkaline magmatic arc associated with closure of the Tornquist Sea basin separating the paleocontinents Avalonia and Baltica (Pharaoh et al., 1993, 1995). The South Leicestershire Diorite Suite and the Mountsorrel Complex (Le Bas, 1972) quarried in the East Midlands were emplaced at 452 +8/−5 Ma (2σ, U-Pb zircon concordia age: Pidgeon and Aftalion, 1978; Noble et al., 1993). These localities lie at the western end of the Derby to St Ives Magnetic Anomaly, associated with a WNW-ESE–trending chain of concealed dioritic bodies (Cornwell and Walker, 1989; Lee et al., 1993) likely occupying a backarc rift. Boreholes in the vicinity of The Wash embayment encountered felsic volcanic and hypabyssal rocks in the pre-Carboniferous basement which previously yielded imprecise U-Pb zircon crystallization ages of 449 ± 13 Ma and 457 ± 20 Ma (2σ), respectively (Noble et al., 1993; Pharaoh et al., 1997). Andesitic lavas (so far undated) are encountered in several other boreholes in the region.(Figs. 2 and 3). For convenience, the Lake District–E England Arc will be subsequently referred to using the acronym LD-EE Arc. The arc magmatic suites studied are associated with underthrusting of Tornquist oceanic lithosphere beneath Avalonia in Mid- to

© 2026 United Kingdom Research and Innovation.

Late Ordovician time at a subduction zone located just offshore, in the vicinity of the Dowsing–South Hewett Fault Zone (Lee et al., 1993; Pharaoh et al., 1993, 1995; Kearey and Rabae, 1996; "Dowsing Suture" on Figs. 1 and 2). The Thor Suture (Berthelsen, 1998) located closer to Baltica (Fig. 1) marks a further, distinct, subduction zone (e.g., Pharaoh, 1999) and may have generated a magmatic arc in the vicinity of the Mid-North Sea High (Williamson et al., 2002). The intervening crust underlying the Mid-North Sea High (colored orange in Fig. 1), differs in structure and geophysical properties to typical crust of Avalonia and Baltica (Lee et al., 1993; Pharaoh, 1999; Williamson et al., 2002; Smit et al., 2016; Crowder et al., 2021) and has been attributed to the Southern North Sea–Lüneberg Terrane (Franke, 1995; Pharaoh, 1999). The affinities of this suspect terrane may lie with Avalonia (Winchester et al., 2002; Cocks and Fortey, 2009), or with immature accreted early Paleozoic crust such as the Ganderia Terrane (van Staal and Barr, 2012).

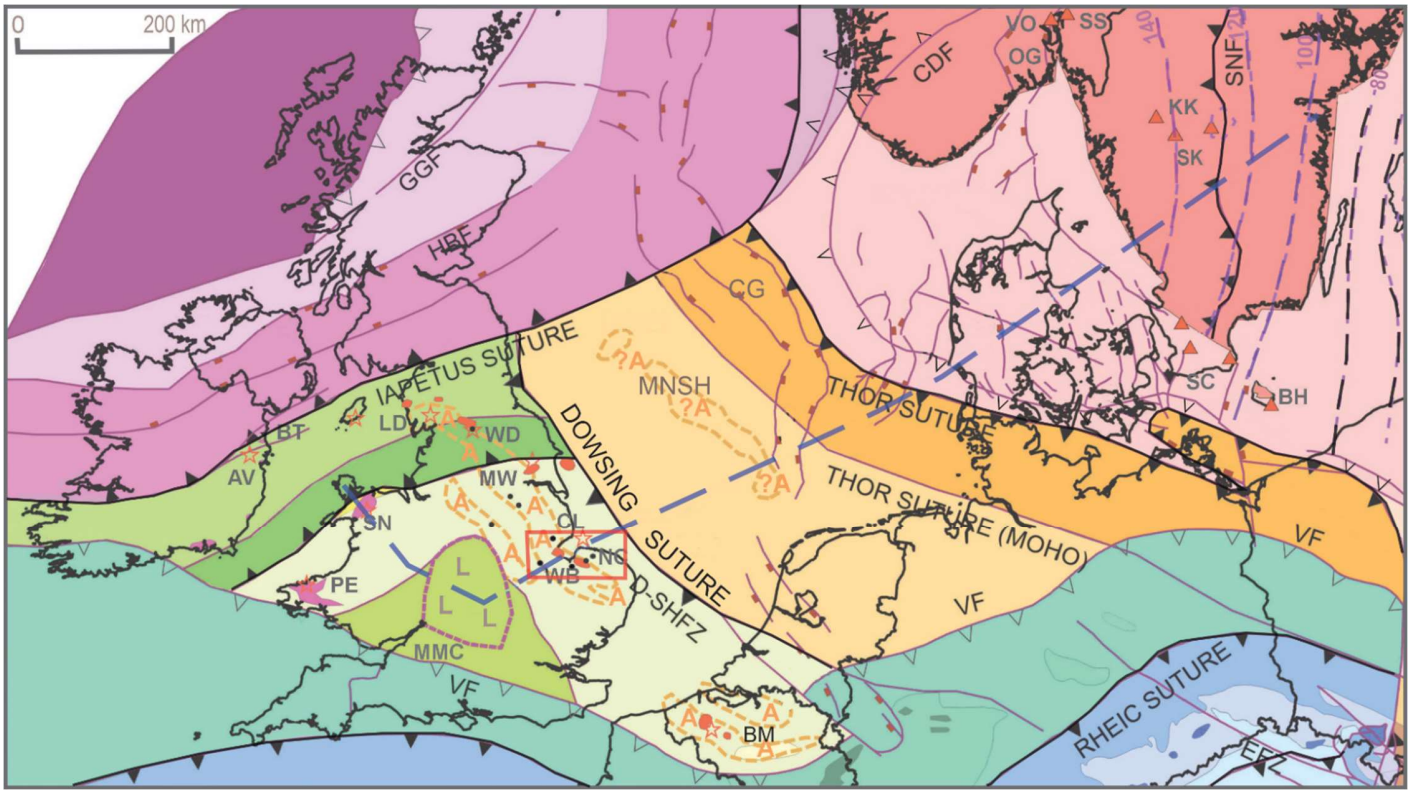

Figure 1. Map of Caledonian basement structure in NW Europe (after Pharaoh, 1999). Contains mapping from ESRI-ArcMap. Major structures: CDF—"Caledonian Deformation Front"; CG—Central Graben; D-SHFZ—Dowsing–S Hewett Fault Zone; EFZ -Elbe Fault Zone; GGF—Great Glen Fault; HBF—Highland Boundary Fault; MMC—Midland Microcraton; MNSH—Mid-North Sea High; VF—Variscan Thrust Front. Terrane elements: Laurentian terranes—purple to mauve shades; "Avalonian Microcontinent"—green shades; "Baltica Continent"—pink shades; "Southern North Sea–Lüneberg Terrane"—orange shades; Variscan Orogen "internide zone"—blue shades. The small red rectangle shows the location of Figures 2 and 4A. The blue dashed line indicates the line of the geotransect lithospheric section shown in Figure 16. Studied boreholes: CL—Claxby 1; NC—N Creake 1. Key localities: BH—Bornholm, Denmark; KK—Mt. Kinnekulle, Mossen, Sweden; SK, Skövde, Sweden; SS—Sinsen, Norway; VO—Vollen, Norway. Other localities: AV—Avoca; BT—Bellewstown Terrane; LD—Lake District; OG—Oslo Graben; PE—Pembrokeshire; SC—Scania, Sweden; SN—Snowdonia (Eryri); SNF, Sveconorwegian Front. Conjectured Late Ordovician arc—orange dashed line, orange "A" and "?A"); lamprophyric intrusions—magenta "L." Preserved thickness contours (in centimeters) for the Kinnekulle Metabentonite (purple dashed lines) after Bergström et al. (1995). Major negative Bouguer gravity anomalies: BM—Brabant Massif; LD—Lake District; MW—Market Weighton; WB—Wash Batholith; WD—Wensleydale.

Sandbian (Late Ordovician) strata in the Scandinavian and peri-Baltic region (Baltoscandia) and the Canada–U.S. Midcontinent region contain numerous horizons of metabentonite (MB) or K-bentonite, the lithified tephra from contemporaneous Plinian eruptions. Two Ordovician tephra associated with possible super-eruptions have been studied in considerable detail (Huff et al., 1992, 1996; Bergström et al., 1995): the up to 2-m-thick Kinnekulle MB (KKMB) or "Big Bentonite," covering at least 690,000 km^2 from Oslo in the west (Fig. 1) to Belarus in the east; and the Millbrig MB, covering

© 2026 United Kingdom Research and Innovation.

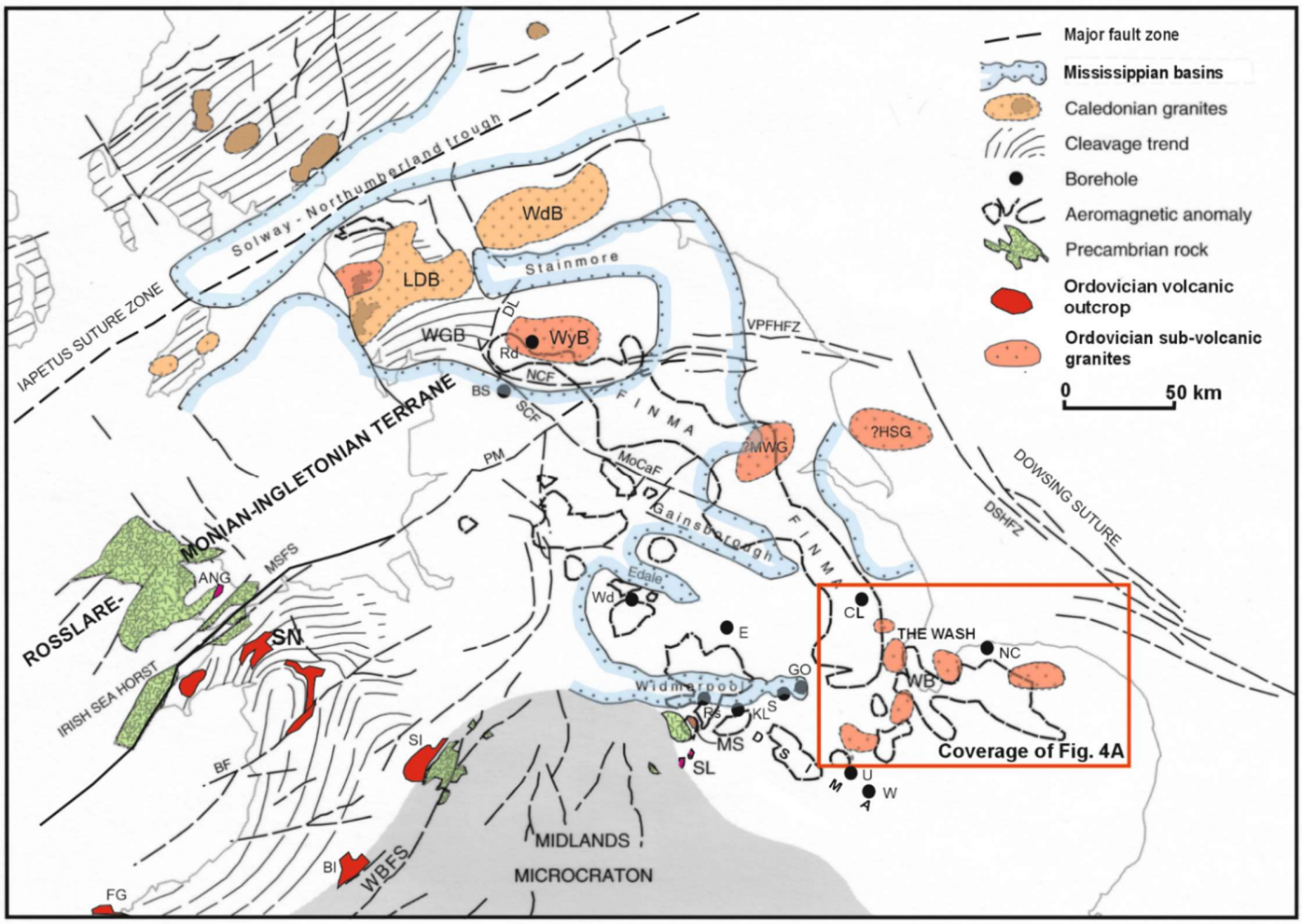

Figure 2. Map of Mid- to Late Ordovician basement structure and magmatic centers in southern Britain, modified from Pharaoh et al. (1997). The red rectangle shows the location of Figure 4A. Borehole locations: BS—Beckermonds Scar; CL—Claxby 1; GO—Great Osgrove Wood; NC—N Creake 1; E—Eakring 146; KL—Kirby Lane; Rd—Raydale; Rs—Rempstone; S—Sproxton; U—Upwood; W—Warboys; WD— Woodale. Other localities: ANG—Anglesey; BI—Builth Inlier; FG—Fishguard; MS—Mountsorrel; SI—Shelve Inlier; SL—S Leicestershire (Croft, Enderby) intrusions; SN—Snowdonia (Eryri); WGB—Windermere Group Basin. Major negative Bouguer gravity anomalies: ?HSG—Inferred Hornsea Granite; LDB—Lake District Batholith; ?MWG—Inferred Market Weighton Granite; WB—Inferred Wash Batholith; WdB—Weardale Granite Batholith; WyB—Wensleydale Granite Batholith. Major positive magnetic anomalies: DSIMA—Derby–St Ives Magnetic Anomaly; FINMA—Furness-Ingleborough-Norfolk Magnetic Anomaly. Tectonic lineaments: BF—Bala Fault; DL—Dent Line; DSHFZ—Dowsing–S Hewett Fault Zone; MoCaF—Morley-Campsall Fault; MSFS—Menai Strait Fault System; NCF—N Craven Fault; PM—Pennine Monocline; SCF—S Craven Fault; VPFHFZ—Vale of Pickering–Flamborough Head Fault Zone; WBFS—Welsh Borderland Fault System.

a large part of the U.S. Midcontinent region. Both have possible dense rock equivalent-volumes exceeding 900 km^3 (Huff et al., 1996), and both are composite, the product of multiple eruptions. These super-eruptions are associated with the Guttenberg $\delta^{13}C$ Isotope Excursion, the first of a series of $\delta^{13}C$ and $\delta^{18}O$ isotope excursions that grew in magnitude through Late Ordovician time (Bergström et al., 2010, 2016), and have been implicated in global climatic change leading to global cooling, glaciation and faunal mass extinction in Hirnantian (latest Ordovician) time (Armstrong, 2007; Buggisch et al., 2010; Sell, 2011). The inference of time-equivalence of these two MBs (Huff et al., 1992; Bergström et al., 1995) was subsequently disproved by mineralogic and chemical studies (Haynes et al., 1995; Sell and Samson, 2011) and increasingly precise radiometric dating (Min et al., 2001; Sell et al., 2013; Bauert et al., 2014). "State of art" ages for the KKMB are U-Pb chemical abrasion–isotope dilution–thermal ionization mass spectrometry (CA-ID-TIMS) zircon dates of 454.41 ± 0.17/0.21 Ma (2σ, Bornholm, Denmark: Sell et al., 2013); 454.52 ± 0.50 Ma (2σ, Vollen, Arnestad, Norway: Svensen et al., 2015): and 454.06 ± 0.43 Ma (2σ, Sinsen, Oslo, Bed #30: Ballo et al., 2019). The Upper Grimstorp MB, lying ca. 5 m above

© 2026 United Kingdom Research and Innovation.

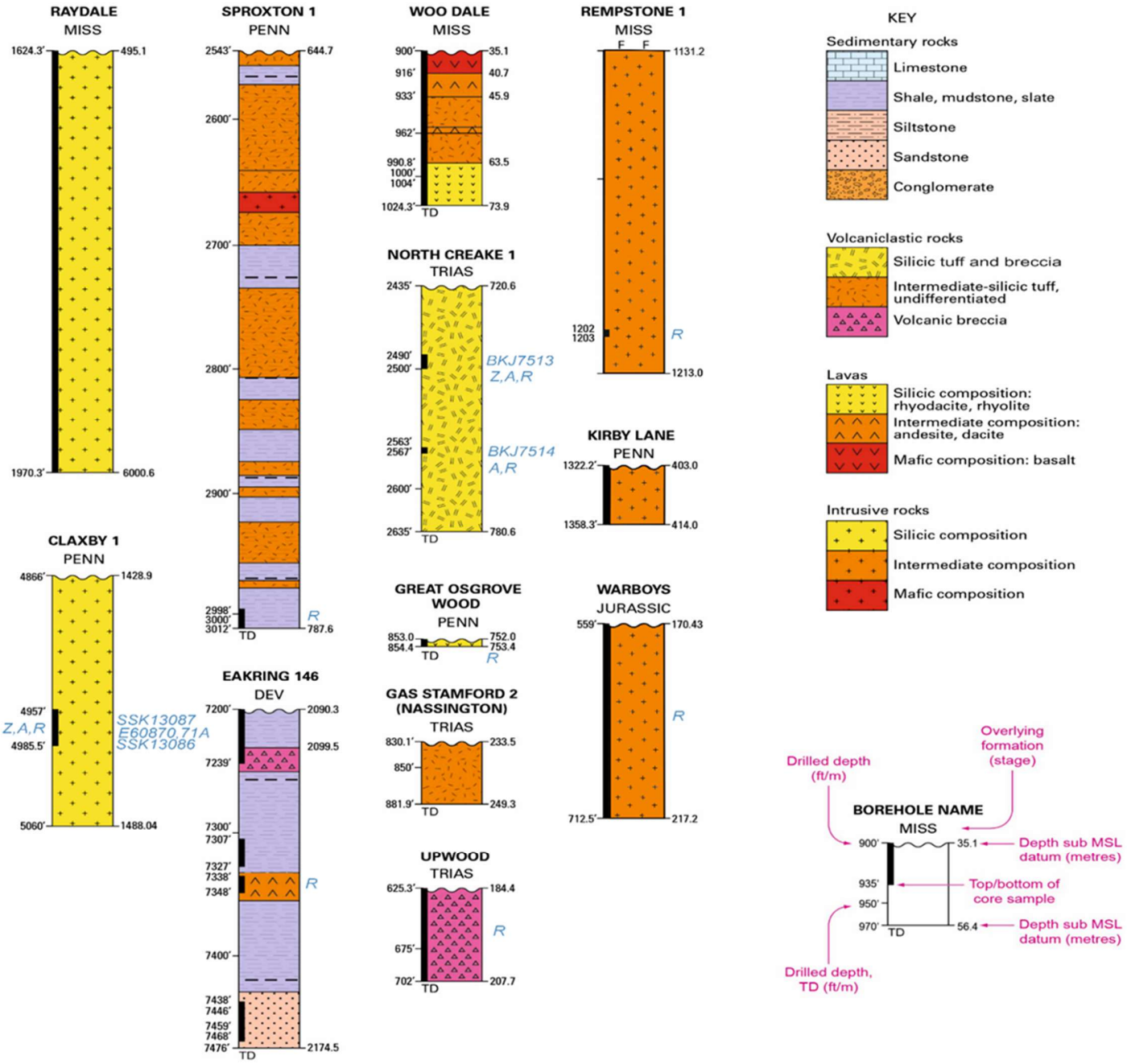

Figure 3. Volcanic and intrusive rocks of Late Ordovician and likely Late Ordovician age penetrated by boreholes in the East Midlands–Wash region of E England. Modified from Pharaoh et al. (1991). Only the Raydale, Claxby 1, and North Creake 1 felsic rocks are securely dated. Sampling points for this study shown in blue italic text: Z—thermal ionization mass spectrometry U-Pb zircon ages; A—Apatite microphenocrysts analyzed by laser ablation–inductively coupled plasma–mass spectrometry (LA-ICP-MS); R—whole-rock samples analyzed by ICP-MS to validate and augment the legacy geochemical data. The diagram emphasizes the small amount of core material available for study. MSL—mean seal level (Ordnance Datum) ; TD–total depth.

the KKMB at Vollen, has yielded a CA-ID-TIMS age of 453.91 ± 0.37 Ma (2σ, Vollen: Svensen et al., 2015) and 453.48 ± 0.74 Ma (2σ, Sinsen Bed #32: Ballo et al., 2019). Antecrysts up to ca. 459 Ma are present in the Sinsen samples. Torsvik and Rehnström (2003) invoked arc magmatism in Avalonia as the likely source of the KKMB, resulting from subduction of Tornquist oceanic crust separating Avalonia (upper plate) and Baltica (lower plate) in Mid- to Late Ordovician time (McKerrow et al., 1991; Cocks and Fortey, 1982). In this paper, we report the results of studies to characterize rock

© 2026 United Kingdom Research and Innovation.

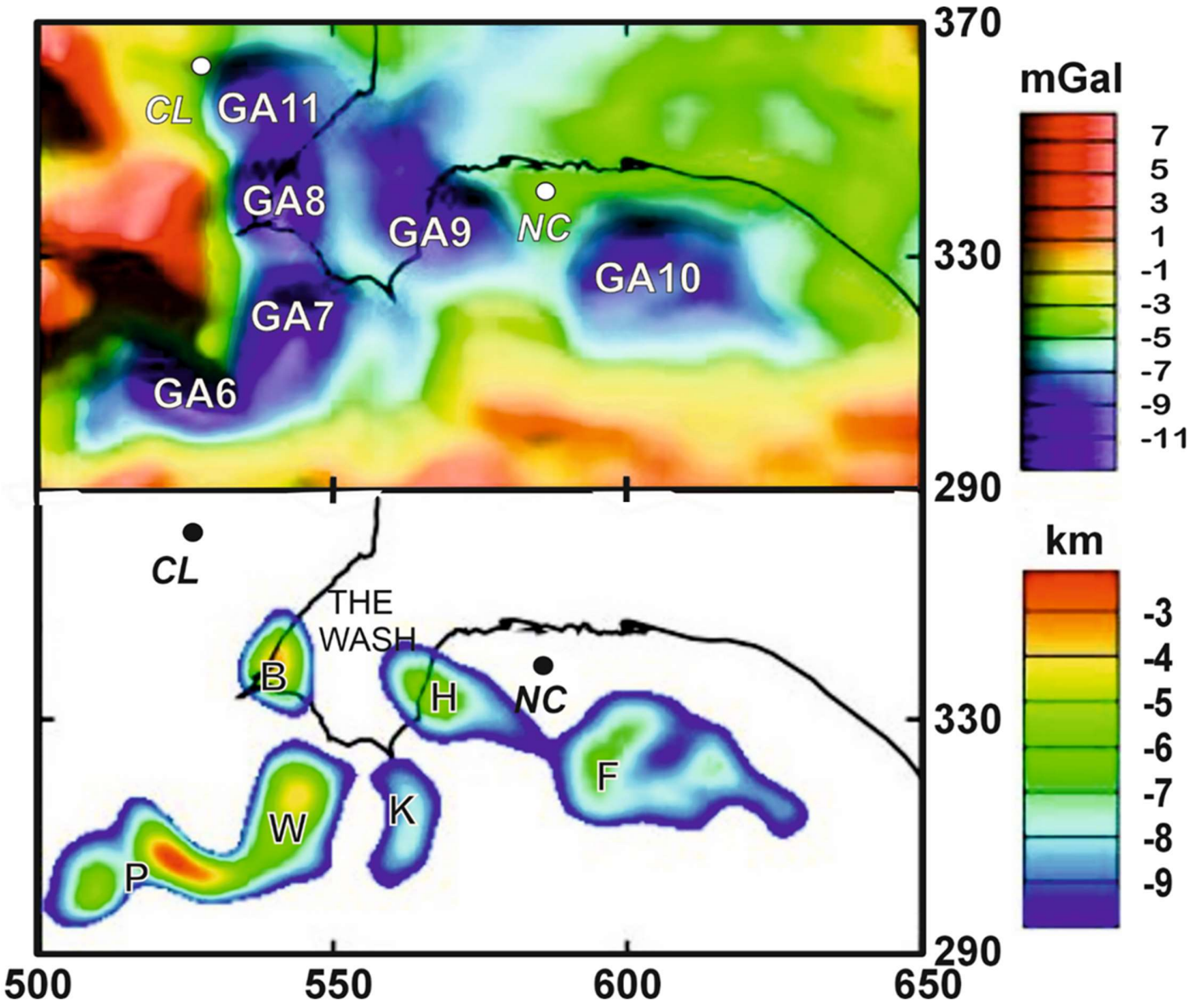

Figure 4. (A) Gravity anomaly map showing significant negative Bouguer gravity anomalies in the vicinity of The Wash (Busby et al., 2006). (B) Depth model assuming a granitic body modelled to 10 km depth (after Busby et al., 2006). Contains mapping from ESRI-ArcMap. Named granite stocks: B—Boston; F—Fakenham; H—Hunstanton; K—King's Lynn; P—Peterborough; W—Wisbech. Boreholes: CL—Claxby 1; NC—North Creake 1.

samples from boreholes on the fringes of the inferred Wash Batholith by generating a state-of-the-art whole-rock geochemical and radiometric database.

- Assess the relationship between the volcanic and inferred plutonic components of the Wash Igneous Complex (WIC) using CA-ID-TIMS U-Pb isotopic data from zircon grains.
- Generate state-of-the-art chemical analyses of apatite microphenocrysts from WIC volcanic components.
- Assess these whole-rock, isotope, and mineral datasets in the context of geochemical correlation of the WIC source with well-studied Sandbian MBs in Baltoscandia.

In doing so we are able to propose, for the first time, a genetic link between the concealed Late Ordovician volcanic rocks buried beneath E England and specific Baltoscandian MBs. All dates cited in this manuscript provide uncertainties at the 2σ level relevant to the comparison being made at the time, following the methodology of Condon et al. (2015). High-precision geochronology dates have three-component uncertainties reflecting analytical, isotopic tracer, and decay constant uncertainties. As such, dates will be presented with one or more uncertainties with the larger of the uncertainties being those

© 2026 United Kingdom Research and Innovation.

which should be used in comparison to the date in question. Where all three uncertainties are presented, the largest of these represents the total uncertainty for the date where these can be used to compare to any date determined by any method.

REGIONAL TECTONIC SETTING; GEOPHYSICAL EVIDENCE FOR THE WASH IGNEOUS COMPLEX

The boreholes studied lie close to significant negative gravity anomalies in the vicinity of The Wash embayment (Figs. 2 and 4). Claxby 1 Borehole (BH) lies beyond the N edge of the anomalies (Fig. 4). The microgranite drilled is interpreted as a high-level, sub-volcanic apophysis of the parent body (Pharaoh et al., 1997). North Creake 1 BH is located to ESE of the gravity anomalies (Figs. 2 and 4) and drilled dacitic tuff-breccias (Fig. 3). A third borehole at Great Osgrove Wood, 50 km W of The Wash (Fig. 2), encountered felsic tuff.

The Wash gravity anomaly comprises a cluster of individual negative (to −11 mGal) Bouguer gravity anomalies (Fig. 4A), associated with stocks overlying a possible concealed granite batholith (Chroston et al., 1987). The modeled volume of the individual stocks (to 10 km depth) ranges from 750 km^3 to 1500 km^3 (Busby et al., 2006) while the total volume is at least 3000 km^3. Thus, putative magma chambers preceding the batholith had sufficient volumetric capacity to supply one or several super-eruptions exceeding 500 km^3(dense rock equivalent). In this paper we demonstrate that the silicic volcanic rocks (and underlying inferred batholithic complex) are components of the Wash Igneous Complex (WIC). Gravity anomalies of similar magnitude but lesser complexity are present in a chain extending NW from The Wash to Market Weighton, in S Yorkshire (Fig. 2) where a conjectured granite (Bott et al., 1978), is also undrilled; to NW Yorkshire, where emplacement of the Wensleydale Granite (Dunham, 1974), has been dated by U-Pb zircon TIMS at 449.21 ± 0.52 Ma (Pashley et al., 2021); and to exposed silicic volcanic and granitic rocks of the southern Lake District (Fig. 2) dated in the range of 452–450 Ma (Hughes et al. 1996; Millward and Evans, 2003). The spatial separation of these proven and putative silicic volcanic/granitic complexes is 100–150 km (Fig. 2).

The silicic complexes occupy apertures in an otherwise unbroken chain of magnetic anomalies (Fig. 2) extending from N England to The Wash, the Furness-Ingleborough Norfolk Magnetic Anomaly (Cornwell and Walker, 1989; Lee et al., 1993). The cause of the latter is attributed to magnetite-bearing metasediments of likely Cambrian age inferred to form the substrate to the Late Ordovician volcanic arc, and the integrity of the Furness-Ingleborough Norfolk Magnetic Anomaly is considered to reflect both the structural trend and continuity of the concealed Caledonide basement in this region. Recently, Waldron et al. (2025) have questioned this inferred integrity, postulating the presence of an Acadian (late Caledonian) age suture which they refer to as the Ynys Môn Line. Such a structure, if it exists, would have significant implications for the inferred continuity of the volcanic arc, and will be discussed later.

SAMPLE DESCRIPTION

The samples analyzed were obtained from legacy borehole cores held in the British Geological Survey. Claxby 1 (Deviated) BH (Figs. 2–4) was drilled for hydrocarbon exploration (BNG TF 2981 6428; BNG locations are converted to latitude and longitude WGS84 values in the Supplemental Material[1]). It encountered 59.13 m of variably altered pinkish-gray granophyric microgranite (Fig. S1; photographs of slabbed and varnished core, and derived photomicrographs are presented in Figs. S1 and S2) overlain by Pennsylvanian strata (Fig. 3) at 1428.9 m depth sub Ordnance Datum (OD, UK sea level datum); 8.69 m of core were recovered. The microgranite is cut by fibrous quartz-calcite veins produced by early hydrothermal alteration and later, post-magmatic brecciation (Fig. S1). Apatite microphenocrysts are small (20–50 µm) and euhedral to suhedral. Anhedral grains associated with this alteration show anomalous cathodoluminescence and are significantly or partially authigenic. North Creake 1 BH (Figs. 2–4; BNG TF 8567 3864), drilled for hydrocarbon exploration, penetrated 60 m of pale greenish-gray heterolithic dacitic crystal-lithic tuff-breccia beneath Triassic cover at 720.6 m sub Ordnance Datum. Two short cores were obtained at ca. 738 m and ca. 758 m depth (Fig. 3). The brown crystal-lithic tuff-breccia (Fig. S1) is unwelded but is tectonically deformed. Partly resorbed and cracked quartz crystals (scanning electron microscopy [SEM] images of quartz phenocrysts are included in Fig. S3) up to 2 mm in diameter, with devitrified melt inclusions (Fig. S2B) and fragments of epidotized and sericitized oligoclase are contained in sheared sericite- and chlorite-rich matrix. Numerous fragments of more mafic composition, up to 3 cm long, are present (Fig. S1B). Felsic fragments exhibit granophyric and perthitic exsolution textures (confirmed by scanning electron microscopy analysis). Both

[1] Supplemental Material. Sample descriptions and photographs of sliced core and derived thin sections; analytical conditions and data tables for whole-rock chemistry, zircon U-Pb isotopic composition, and apatite microphenocryst chemistry. Please visit https://doi.org/10.1130/GSAB.S.32048511, to access the supplemental material; contact editing@geosociety.org with any questions.

© 2026 United Kingdom Research and Innovation.

are interpreted as extraclasts. The rock is interpreted as a heterolithic, chaotic tuff-breccia. It originated either as a pyroclastic lag breccia or a caldera collapse breccia (e.g., Lipman, 1999). Apatite microphenocrysts are unaltered, rarely cracked euhedral to subhedral grains ranging in size from 50 μm to 100 μm (SEM and cathodoluminescence [CL] images of the apatite microphenocrysts are included in Fig. S4). Great Osgrove Wood 1 BH, drilled for coal exploration (BNG SK 9652 2460), is located 20 km W of the WIC (Figs. 2 and 3). A very short (1.4 m) core was obtained beneath Pennsylvanian cover at 752.0 m OD (Fig. 3) . The core comprises a tectonically undeformed pale greenish-gray felsic rock containing both fragmental and fluidal textures, including flowage folds (Fig. S2C and S2D). It is interpreted as a rheomorphic ash flow of rhyolitic composition, provisionally assigned to outflow from WIC.

METHODOLOGY/ANALYTICAL PROCEDURES

In the current project, the drill cores were resampled (Fig. 3) and analyzed in the laboratories of the British Geological Survey at Keyworth, Nottingham, UK, using procedures described in the Supplemental Materials.

- "Whole-rock" analyses were undertaken by inductively coupled plasma–mass spectrometry (ICP-MS) A small number of legacy powdered samples previously analyzed by X-ray fluorescence (XRF) and instrumental neutron activation analysis (INAA) were reanalyzed by ICP-MS, to ensure the veracity of the original dataset. This generated a high-precision dataset of some 50 elements per sample (Table S1; data tables for geochemical and isotopic data are presented in the Supplemental Materials).
- Zircon grains were separated from the Claxby BH core at 4973 ft (1515.8 m: SSK113087) and 4983 ft (1518.8 m: SSK113086) depth (Fig. 3). For N Creake BH, a legacy zircon separation from the study by Noble et al. (1993), was available. The zircon grains were analyzed using thermal ionization mass spectrometry (CA-ID-TIMS) following chemical abrasion procedures (Mattinson, 2005). Analytical procedures and data are listed in the Supplemental Materials (U-Pb analyses by TIMS are listed in Table S2).
- Polished 100-μm-thick microscope slices, ~2 × 3 cm in size, were investigated by cathodoluminescence (CL) and scanning electron microscopy to identify grains and their relationships. Apatite grains were identified, their grain morphology classified and mapped on optical images (Fig. S5). Two 100-μm-thick probe slides (BKJ7513X1 and BKJ7514A) were prepared for the N Creake samples; and two slides (E60870A, E60871A) were prepared for the Claxby samples (Fig. 3). These numbers refer to the borehole and petrographic registered collections of the British Geological Survey.The thickness of the slide increases the stability of both slide and crystals during ablation and increases the chances of apatite crystals having a thickness >30 μm, thereby enabling longer ablation times.
- The apatite grains on the polished slides were analyzed by laser ablation (LA)-ICP-MS to provide geochemical data for the following elements: Al, Fe, Mn, Mg, P, Pb, Sr, Th, U, Y and rare earth elements (REEs; geochemical data for apatite microphenocrysts are presented in Table S3). Detection limits and precision are provided in the Supplemental Material.

INTERPRETATION OF WHOLE-ROCK GEOCHEMICAL DATA; CLASSIFICATION AND TECTONIC SETTING

The whole-rock geochemical data generated by ICP-MS are summarized and interpreted via multi-element diagrams (Fig. 5) and in bivariate cross-plots (Fig. 6).

ICP-MS data from mafic and intermediate components of the E Midlands plutonic and volcanic suites are depicted in Figure 5A. Although undated so far, these samples exhibit pristine igneous textures, are tectonically undeformed, and thus are unlikely to be of Precambrian age. The borehole locations are shown in Figure 2 and generalized borehole logs in Figure 3. The most primitive samples are basaltic and basaltic andesite clasts from Upwood BH. The geochemical patterns are more primitive than N-MORB and flat through the heavy rare earth elements (HREE) toward P. There is a small negative Eu anomaly indicating minor fractionation of plagioclase. The geochemical pattern then rises through the light rare earth elements (LREE) e.g., La and Ce, before a significant depletion of Nb and Ta, likely reflecting preferential retention of titanomagnetite and/or rutile in the subducting plate and the overlying hydrated mantle source region (Pearce, 1983). Beyond Ta, large ion lithophile elements (LILE) such as K, Rb, and Ba are significantly enriched compared to N-MORB, due to dehydration of the subducting slab. These characteristics are typical of continental arc volcanism (Pearce, 1983; Pharaoh et al., 1993). The most primitive, mafic diorite sample from the Warboys BH follows a parallel but more enriched pattern, which is further enhanced through increasingly silicic intermediate compositions. A small divergence of the patterns here may also reflect a component of crustal contamination.

© 2026 United Kingdom Research and Innovation.

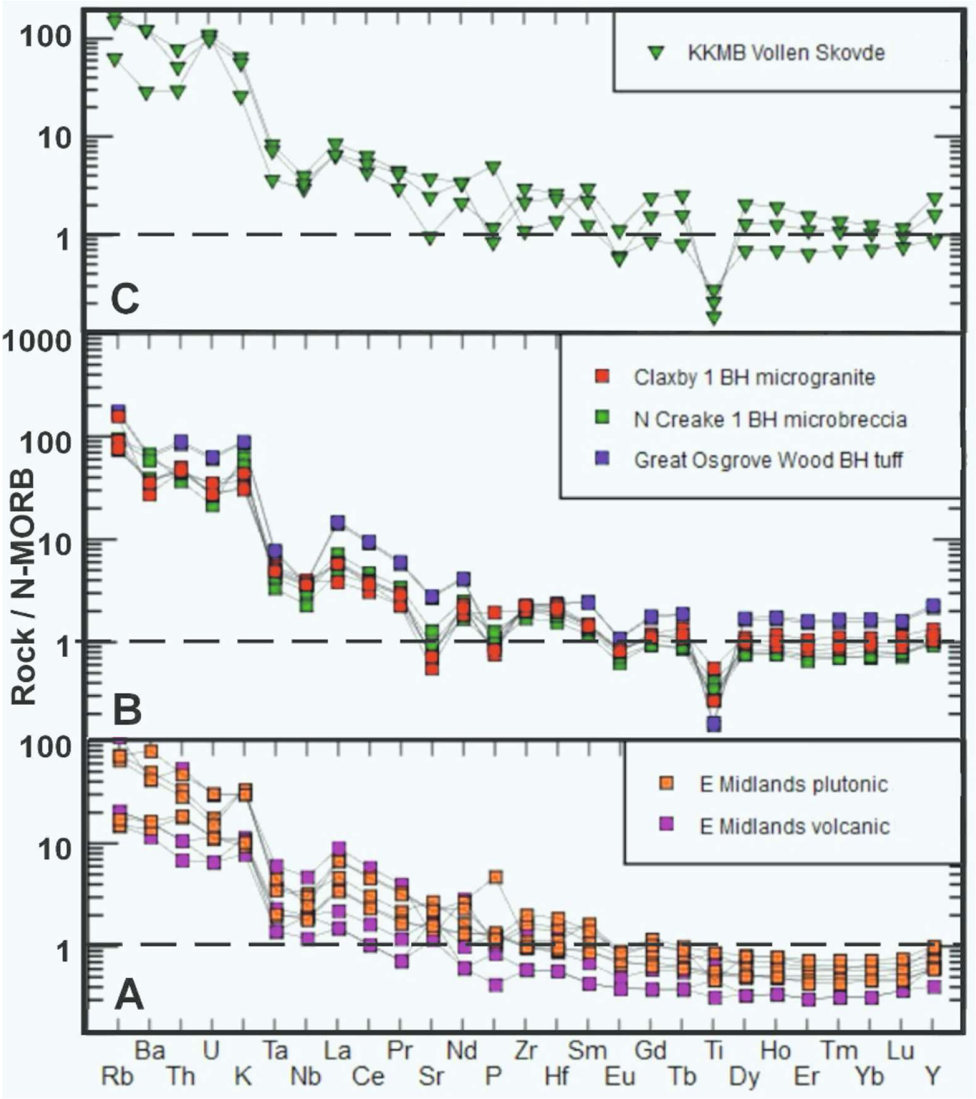

Figure 5. Multi-element diagrams (spidergrams) for selected whole-rock inductively coupled plasma–mass spectrometry data from the Sandbian magmatic complexes in E England shown in Figure 3, and comparative whole-rock analyses for the Kinnekulle Metabentonite (KKMB) from Norwegian and Swedish localities. Concentrations are normalized to normal mid-ocean-ridge basalt (N-MORB) values (Hofmann, 1988). (A) Selected data from the Upwood borehole (BH; basaltic-andesite volcanic clasts) and the sill proved by Warboys BH (mafic diorite). (B) Silicic components of the Wash Igneous Complex. (C) Representative whole-rock samples of KKMB from the Vollen, Oslo and Skövde, Västergotland localities. Data and locality information listed in Supplemental Materials (see text footnote 1).

Geochemical data from the three felsic components of the WIC are plotted in Figure 5B. Their geochemical patterns are broadly parallel to those shown in Figure 5A, but represent a further step in magmatic evolution by fractionation of ferromagnesian minerals. In addition, a prominent depletion of Ti reflects fractionation of titanomagnetite, and minor P, Eu, and Sr depletions reflect fractionation of apatite and plagioclase, respectively. The depletion of Nb and Ta previously recognized as a primary characteristic of the source region is retained and is of slightly greater amplitude. Further enrichment of LILE is observed. In Figure 5C, ICP-MS whole-rock geochemical data for samples from the KKMB at Vollen, Arnestad, Norway, and Skövde, Sweden, are plotted. No correction for diagenetic effects, of the type recommended by Kiipli et al. (2010, 2014a) has been applied to these analyses. Nevertheless, the similarity of the KKMB geochemical patterns to those of the WIC felsic samples (Fig. 5B), in terms of the normalized abundances, the general shape of the patterns, and in detail, the position and magnitude of their anomalies, is striking.

© 2026 United Kingdom Research and Innovation.

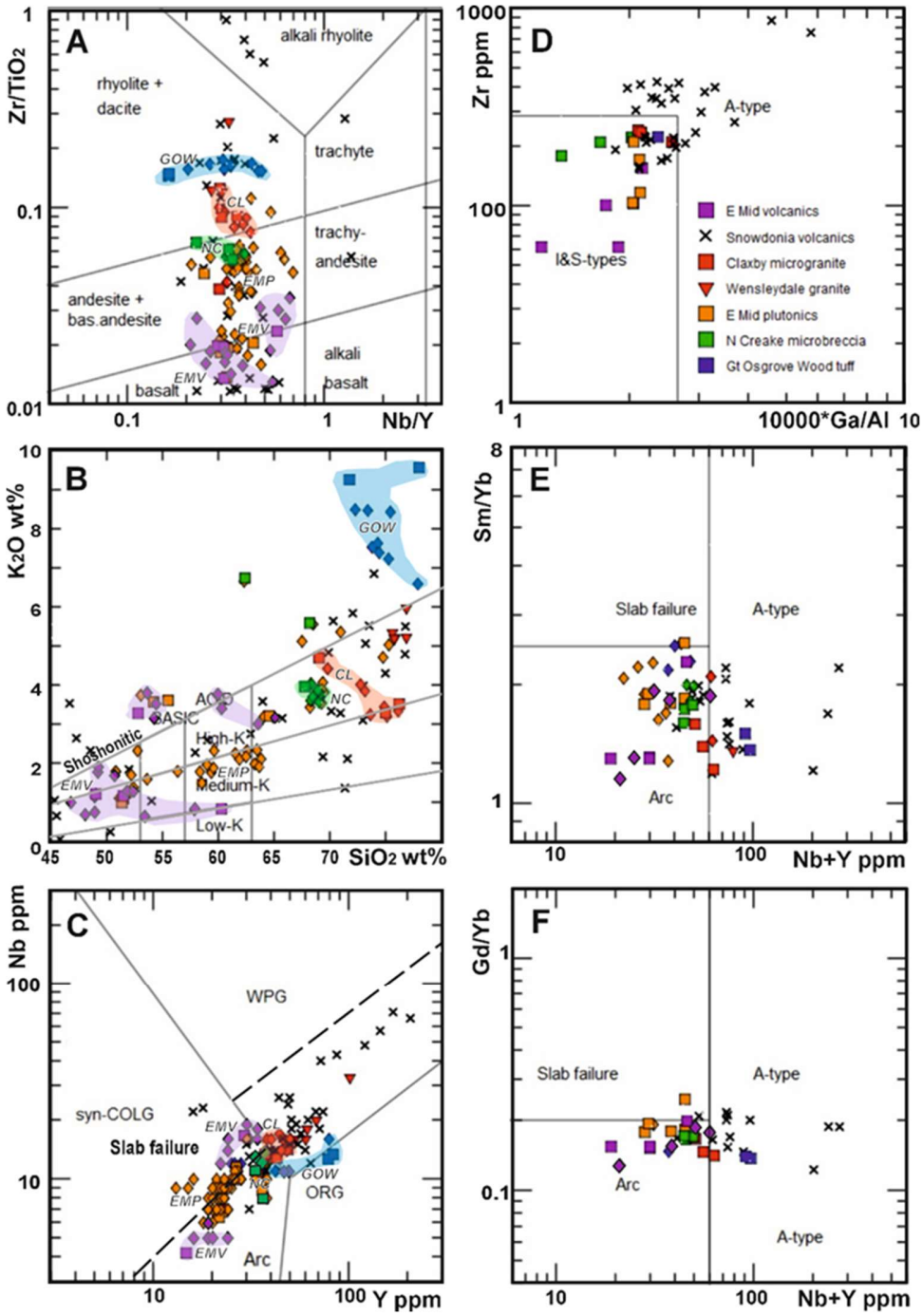

Figure 6. Rock classification and granite discrimination diagrams for Sandbian components of the Wash Igneous Complex proved by deep boreholes in the vicinity of The Wash; East Midland plutonic intrusions (Mountsorrel, S Leicestershire diorites and Rempstone-Melton intrusion); and rhyolitic intrusions and tuffs from the Llewelyn and Snowdon Volcanic Groups of Snowdonia, N Wales. Legacy whole-rock geochemical data analyzed by X-ray fluorescence (major, trace elements) and instrumental neutron activation analysis (REE+Hf+Ta) published by Webb and Brown (1989), Pharaoh et al. (1991, 1993, 1997), and Howells et al. (1991), are shown with small diamond symbols. New inductively coupled plasma–mass spectrometry data are shown with slightly larger square symbols in the same color. (A) Zr/TiO_2-Nb/Y diagram for rock classification. Fields from Pearce (1976). (B) K_2O vs. SiO_2 diagram, with fields for low-, medium-, and high-K series after Gill (1981). (C) Nb-Y diagram for classifying granitic rocks, after Pearce et al. (1984) with additional field boundary (dashed line) separating arc and slab-failure granites from Whalen and Hildebrand (2019). Abbreviated field names: ORG—Ocean Ridge Granites; COLG—collision-related granites; WPG—within-plate granites. (D) Zr-10000 × Ga/Al diagram for granite classification (Whalen et al., 1987). (E) Sm/Yb vs. Nb+Y diagram for tectonic environment of granites (Whalen and Hildebrand, 2019). (F) Gd/Yb vs. Nb+Y diagram for tectonic environment of granites (Whalen and Hildebrand, 2019)

© 2026 UNITED KINGDOM RESEARCH AND INNOVATION.

Classification and Discrimination Diagrams

All of the available geochemical data from the E Midlands - Wash region are plotted in magma characterization and discrimination diagrams in Figure 6. Legacy XRF and INAA analyses are plotted with a small diamond symbol of the same color as the new ICP-MS data (larger squares). With the exception of Figure 6B, these diagrams are based on less mobile trace elements, and widely used in the literature. Published data for selected samples from the Llewelyn and Snowdon Volcanic groups of Snowdonia (Eryri), N Wales (Fig. 2), interpreted as the contemporaneous backarc (Kokelaar et al., 1984; Howells et al., 1991) of the LD-EE Arc system, are also included, for comparative purposes, as Plinian eruptions from smaller silicic calderas in the backarc basinal region could also contribute to Sandbian tephra in Baltoscandia.

In Figure 6A, the samples from N Creake and Claxby BHs are of andesitic-dacitic and rhyolitic composition respectively. The Great Osgrove Wood samples are the most evolved (rhyolitic) compositions, resembling evolved peralkaline rhyolites from Snowdonia in their elevated Zr/TiO_2 ratio (Fig. 6A). Samples from all 3 WIC boreholes lie at the felsic end of a medium to high-K calc-alkaline differentiation trend extending from basaltic andesite through andesite, as previously identified on the Irvine and Baragar (1971) FMA (iron-magnesium-alkalis) triangular diagram (Pharaoh et al., 1993, and fig. 3 therein). Figure 6B is the variant of the potash vs silica diagram presented by Gill (1981), albeit used with caution surrounding the possible mobility of the major element oxides. Most of the WIC and other E England volcanic samples plot in the medium-K and high-K calc-alkaline fields. A few analyses plot in the shoshonitic field but these exceptions are considered to be a result of intense alteration of some of the S Leicestershire plutonic rocks. Within WIC, the most significantly altered rocks are the samples from the Great Osgrove Wood BH, a very short basement penetration likely affected by sub-Pennsylvanian unconformity weathering effects. In the Nb-Y diagram of Pearce et al. (1984), modified by Whalen and Hildebrand (2019; Fig. 6C), the WIC felsic rocks plot dominantly in the arc field close to the boundary with the slab-failure field, while some of the Claxby and Great Osgrove Wood BH samples lie in the immediately adjacent field of within-plate granite transitional to ocean ridge granite, as previously identified by Pharaoh et al. (1997). The highly evolved peralkaline rhyolites and comendites from Snowdonia (Howells et al., 1991) with high Zr, Nb, and Y content, plot farther into this transitional field, as do some Great Osgrove Wood samples. Some of the legacy samples plot in the slab-failure field (Fig. 6C), but all the new LA-ICP-MS data plot entirely within the arc field in the analogous Ta-Yb diagram (not shown here). Figure 6D confirms the I-(igneous)/S-(sedimentary) type nature of the felsic WIC magmas, only the peralkaline Snowdon samples plotting in the field of A-type (alkalic) granites. This diagram is used to screen the dataset for alkalic compositions, as recommended by Whalen and Hildebrand (2019), although their full screening protocol e.g., using the Aluminum Saturation Index, has not been implemented because our dataset is incomplete for some major elements (Na) and because Si has likely been mobile. Two further examples of the classification diagrams of Whalen and Hildebrand (2019) help to resolve the ambiguity shown by Figure 6C. These diagrams are based on a very large (>2500 sample) database of high quality (ICP-MS) analyses of granite samples for which the tectonic environment is well constrained. Figures 6E and 6F confirm that all the samples for which REE analyses of good quality are available, plot in the arc-related field, and are not related to slab-failure. Highly evolved Snowdon rhyolitic compositions are of alkalic type, as are two of the Great Osgrove Wood samples. The Sr/Y ratio is a good indicator of the tendency of felsic magmas to evolve toward adakitic compositions and associated porphyry-type mineralization (Nathwani et al., 2020). The Sr/Y ratio of the WIC samples is <30, significantly less than the value of 50, recognized by these authors as the lower threshold for possible porphyry-type or adakitic magmatic associations.

The following summarizes the whole-rock geochemical interpretations for WIC and related suites in the E Midlands and contemporaneous suites in Snowdonia.

- Validated by the new ICP-MS data, the legacy dataset of XRF and INAA analyses can be used with confidence in our interpretation alongside the new data.
- Geochemical patterns and bivariate discrimination diagrams support the previous assignment by Pharaoh et al. (1993) of the magmatic rocks from the WIC and the E Midlands to medium/high-K calc alkaline series.
- The felsic rocks do not show adakitic tendencies nor susceptibility to porphyry-type mineralization.
- The Claxby samples are more evolved than those from N Creake. The Great Osgrove Wood samples are the most evolved, but may have suffered mobilization of alkali elements due to sub-unconformity weathering effects.
- Basaltic components of the backarc basin in Snowdonia cannot be readily distinguished from the WIC rocks on the basis of the diagrams mentioned in the previous paragraphs but the evolved felsic component of the bimodal magmatic system, expressed as peralkaline rhyolites with comenditic tendencies can be.
- The WIC dataset exhibits the key geochemical characteristics of a calc-alkaline magmatic series generated above an active subduction system. The case for a relationship to slab-failure is weak.

© 2026 United Kingdom Research and Innovation.

INTERPRETATION OF CA-ID-TIMS ISOTOPIC DATA

U-Pb isotopic (CA-ID-TIMS) data from the Claxby BH samples yield a weighted mean zircon crystallization age of 454.40 ± 0.11/0.22/0.53 Ma (Sandbian, Late Ordovician; n = 7, mean square of weighted deviates [MSWD] = 0.48; Fig. 7), interpreted as the age of intrusion of the subvolcanic Claxby Microgranite. An outlier date of 456.68 ± 0.26 Ma ($^{206}Pb/^{238}U$ date on a single crystal) is possibly antecrystic. The texturally complex N Creake BH sample hosts two grain populations. An older population of grains yielding a crystallization age of 454.45 ± 0.13/0.23/0.54 Ma (Sandbian, Late Ordovician; n = 6, MSWD = 1) is identical within the analytical uncertainties to the crystallization age from Claxby BH and considered to reflect the same magmatic event.

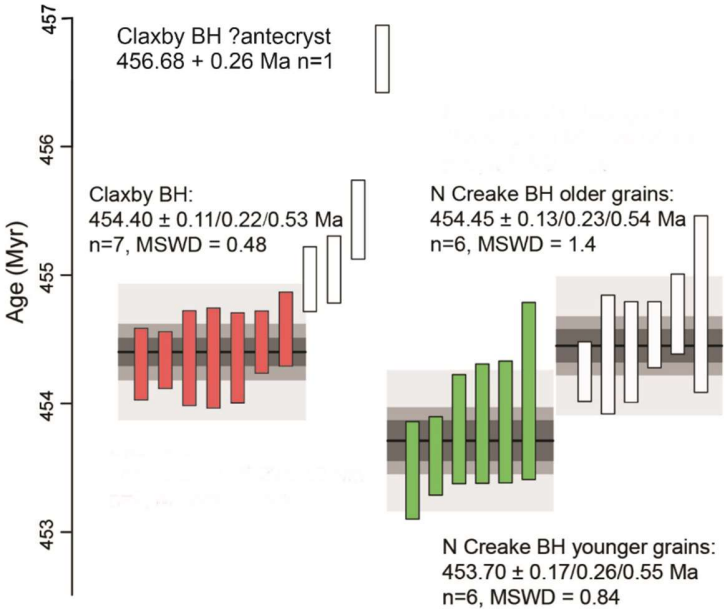

Figure 7. Weighted mean plots of $^{206}Pb/^{238}U$ dates by chemical abrasion–isotope dilution–thermal ionization mass spectrometry for zircon grains separated from core samples from Claxby 1 BH (borehole), Lincolnshire (granophyric microgranite) and North Creake 1 BH, Norfolk (heterolithic felsic tuffaceous microbreccia). The zircon grains in the North Creake sample are inferred to belong to two populations based on their mean square of weighted deviates (MSWD) and the ages calculated accordingly.

The ages have much greater precision than ages previously published (Noble et al., 1993). A younger population of grains from N Creake yields an age of 453.70 ± 0.17/0.26/0.55 Ma (Sandbian, Late Ordovician; n = 6, MSWD = 0.84), interpreted as the age of a magmatic reactivation of the breccia. The close similarity of the crystallization ages from two boreholes located 65 km apart indicates a continuity of the caldera system (and its underlying magma chamber) across this distance. As described in the previous section, the whole-rock geochemical data support the possibility of magmatic consanguinity.

The new ages from components of the WIC of E England are compared with published TIMS zircon ages for felsic magmatic rocks in N England, Wales, and Ireland in Figure 8. Two CA-ID-TIMS zircon ages for the eruption of the Lower and Upper Rhyolitic Tuff formations of Snowdonia (Fig. 2) published by Lusty et al. (2017) are identical to each other and the WIC dates within their analytical uncertainties, but very slightly older than the younger N Creake felsic breccia date (see Fig. 8). These ash flow tuffs of the Snowdon Volcanic Group are the product of Plinian eruptions in the backarc basin (Howells et al., 1991) and thus had the potential to contribute tephra contemporaneous with a WIC arc source. The new WIC TIMS ages are possibly slightly older than the most precise published ages for the Borrowdale Volcanic Group and associated plutonic rocks of N England. The latter typically have 2σ uncertainties of 1–4 m.y., so age equivalence with WIC and Snowdonia cannot be discounted, particularly as the biostratigraphic constraint by marine shales of the *Dicranograptus clingani* biozone (Katian, 453 ± 0.7 Ma to 445.2 ± 1.4 Ma; Cohen et al., 2013) is the same in both Lake District and Snowdonia (Molyneux et al., 2023). Figure 8 also includes CA-ID-TIMS zircon ages for Sandbian MB in Baltoscandia, mostly from the Sinsen, Oslo succession (Ballo et al., 2019). The Kinnekulle Metabentonite (KKMB) is designated "Bed 30" in a dominantly mudstone succession, which also includes underlying (Grefsen, Sinsen) and overlying (Grimstorp) MBs (Figs. 8 and 9).

© 2026 United Kingdom Research and Innovation.

Figure 8. Chronostratigraphic chart for Sandbian time, with published ages of the highest precision for magmatic rocks in E Avalonia (England, Wales, Eire), Baltoscandia, and Laurentia (Midcontinent region of United States and Canada). Stage boundary ages after International Chronostratigraphic Chart (Cohen et al., 2013) Circles indicate biotite Ar/Ar data, diamonds are garnet Sm-Nd analyses and bars denote zircon U-Pb analyses. Black and gray bars represent the analytical uncertainty associated with U-Pb analyses performed using an EARTHTIME isotopic tracer (Condon et al., 2015; McLean et al., 2015) or other in-house tracers respectively. White bars indicate additional systematic uncertainty component related to the ^{238}U decay constant (all U-Pb analyses) and isotopic tracer calibration (for EARTHTIME tracer only). SIMS—sensitive ion mass spectrometry; BH—borehole; n—number of single crystal analyses included in each U-Pb date calculation; bulk—analyses on multigrain zircon fractions. U.S. states: KY—Kentucky; MO—Missouri; OK—Oklahoma; TN—Tennessee. Abbreviations: SMB—Grefsen MB at Sinsen locality; KKMB—Kinnekulle MB; UGMB/LGMB—Upper/Lower Grimstorp MB; BVG—Borrowdale Volcanic Group; SVG—Snowdon Volcanic Group; CKG—Croghan Kinshelagh Granite; WMB—Womble MB; DMB—Deicke MB; MMB—Millbrig MB. References cited: 1—Thirlwall and Fitton (1983); 2—Kunk and Sutter (1984); 3—Tucker and McKerrow (1995) with further work by Compston (2000) and Compston and Gallagher (2012); 4—Evans et al. (1995); 5—Hughes et al. (1996); 6—Min et al. (2001); 7—Millward and Evans (2003); 8—Sell et al. (2013); 9—Svensen et al. (2015); 10—Lusty et al. (2017); 11—Fritschle et al. (2018); 12—Ballo et al. (2019); 13—Metzger et al. (2021); 14—Pashley et al. (2021); 15—Oruche et al. (2018). Except for the analyses of Fritschle et al. (2018) all other U-Pb work cited here was carried out by isotope dilution–thermal ionization mass spectrometry.

© 2026 United Kingdom Research and Innovation.

The new WIC ages are identical within the analytical uncertainties to the CA-ID-TIMS ages 454.41 ± 0.17 Ma for the KKMB published by Sell et al. (2013; Vasagård, Bornholm, Denmark) and 454.52 ± 0.50 Ma by Svensen et al. (2015; Vollen, Arnestad, Norway) as well as the TIMS age of 454.06 ± 0.43 Ma published by Ballo et al. (2019; Sinsen, Norway). They are comparable to the Ar-Ar age of 454.8 ± 2.0 Ma published by Min et al. (2001; Kinnekulle, Sweden); and comparable to less precise LA-ICP-MS zircon U-Pb ages published by Bauert et al. (2014). The age derived from the younger grain population in North Creake is identical within isotopic tracer calibrated uncertainty (453.70 ± 0.17/0.26 Ma) to the TIMS ages of 453.48 ± 0.74 Ma and 453.91 ± 0.37 Ma for the Lower (Sinsen Bed #31) and Upper (Sinsen Bed #32) Grimstorp metabentonites (Fig. 9), respectively (Ballo et al., 2019; Svensen et al., 2015).

Also shown on Figure 8 are precise zircon U-Pb TIMS data for the Midcontinent region of the United States and Canada. The median of these ages are ca. 453.5 Ma for the Deicke MB and 453.36 Ma for the overlying Millbrig MB, with 2σ analytical uncertainties of 0.12–0.54 m.y., slightly younger than the WIC and KKMB ages cited in the previous paragraphs .

BALTOSCANDIAN TEPHRA OF SANDBIAN AGE

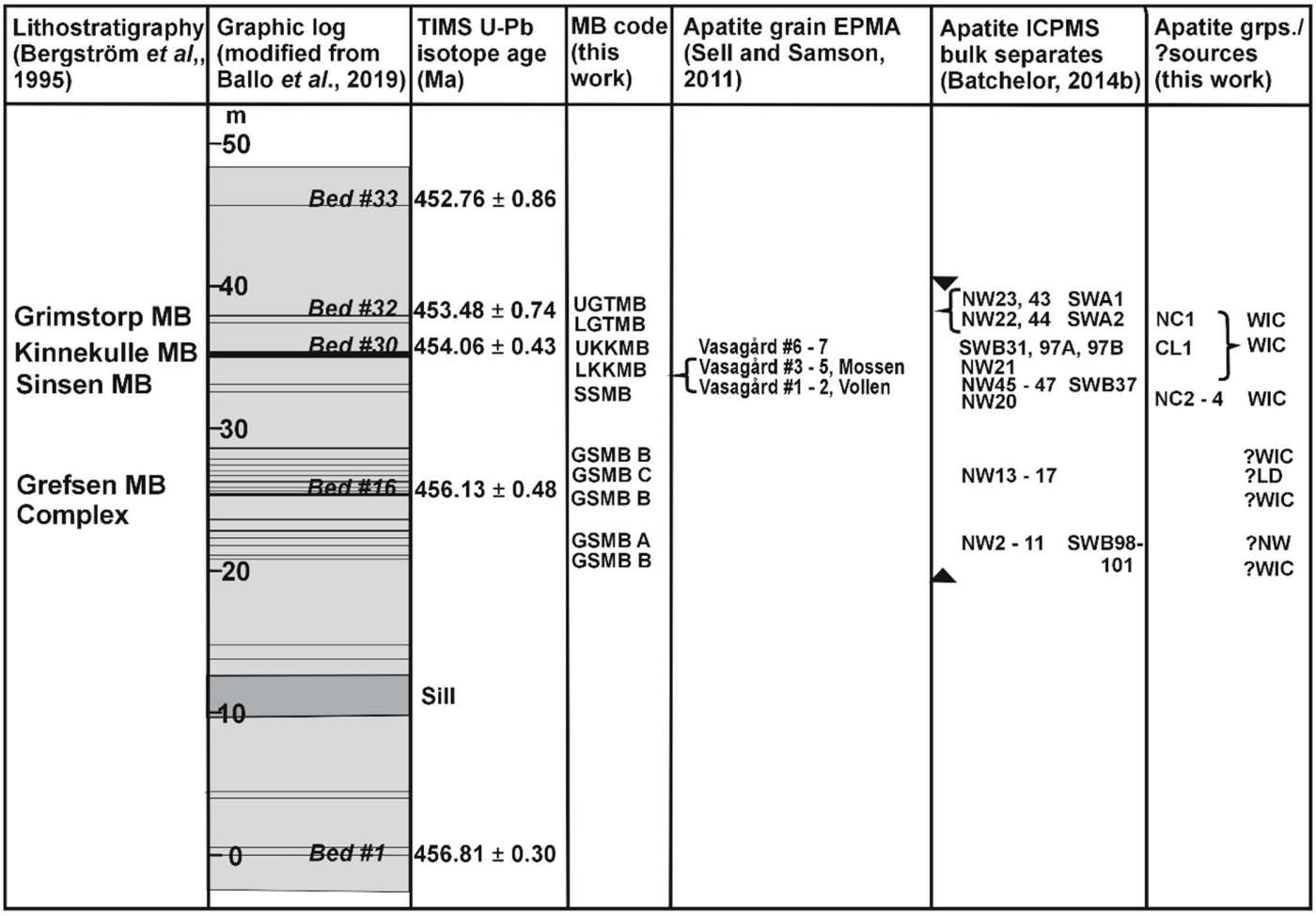

Figure 9. Stratigraphic log for the Arnestad Formation at the Sinsen, Oslo, Norway, locality (modified after Ballo et al., 2019). Lithostratigraphic nomenclature follows Bergström et al. (1995). The 20 m section sampled by Batchelor (2014b) lies between 20 m and 40 m on the scale. The position of samples analyzed for this study, and legacy apatite microphenocryst analyses by electron probe microanalysis (EPMA data, Bornholm, Denmark, Norway and Sweden; Sell and Samson, 2011 and bulk separate analyses by inductively coupled plasma–mass spectrometry (ICP-MS; Batchelor, 2014b), is shown. Samples from the Vollen and Sinsen, Norway, localities are prefixed NW; samples from correlative horizons in Sweden are prefixed SW. Key to abbreviations: GSMB A—Grefsen Group A; GSMB B—Grefsen Group B; GSMB C—Grefsen Group C; SSMB—Sinsen MB; L/UKKMB—Lower/Upper Kinnekulle MB; L/U GTMB—Lower/Upper Grimstorp MB; LD—Lake District; NW—North Wales; WIC—Wash Igneous Complex; MB—metabentonite.

© 2026 UNITED KINGDOM RESEARCH AND INNOVATION.

Metabentonite horizons are extensively developed in the Sandbian strata of Baltoscandia and the East European Platform, covering an area in excess of 690,000 km^2 (Huff et al., 1996). Most are relatively thin, with a thickness of a few centimeters. The stratigraphic nomenclature for the Arnestad Formation (Fig. 9) of the Oslo region was established by Bergström et al. (1995). Four groups of MBs are recognized. The lower part of the formation comprises a sequence of up to 27 relatively thin (centimetric) MBs of the Grefsen complex, some grouped (Fig. 9), overlain by one or two thin Sinsen MBs. The Kinnekulle MB, locally up to 2 m in thickness in its type area on Mount Kinnekulle, near Mossen in Västergotland, Sweden (Fig. 1) is probably composite (Sell and Samson, 2011; Batchelor, 2014b, and is recognized from Oslo eastward to Belarus, a distance of at least 900 km. It has a total estimated dense rock equivalent volume of at least 972 km^3 (Huff et al., 1996). The thin Grimstorp MBs lie a few meters above the KKMB. Bergström et al. (1995) have correlated the Oslo sequence to the shale-dominated succession in Skåne (Sularp Formation) and Bornholm, and the carbonate-dominated sequence typical of the type-area in Västergotland (Dalby Formation).

The new CA-ID-TIMS U-Pb zircon age for the most widespread and, presumably, most catastrophic magmatic event in the WIC at ca. 454.4 Ma are identical within analytical uncertainties to the most precise published ages for the KKMB, as noted in the previous section. A less widespread and less catastrophic event at ca. 453.7 Ma, associated with collapse of the WIC caldera, is identical within analytical uncertainties to one or other of the Grimstorp MB beds, as notedin the previous section. Other potential Avalonian sources for Baltoscandian MB, constrained by TIMS U-Pb zircon data, are the Lower and Upper Rhyolitic Tuff formations of Snowdonia, erupted at ca. 454.4 Ma (Lusty et al., 2017), and the Borrowdale Volcanic Group in the Lake District (Fig. 2).

The Arnestad Formation MBs in the Sinsen section were the subject of detailed geochemical studies by Batchelor (2014b), who published major and trace element XRF data for whole-rock samples, and more limited ICP-MS trace element data (Sr, Y, Th, U, and REE) for apatite bulk separates. More comprehensive whole-rock major and trace element data (including REE) were published for the correlative Sularp Formation in the Röstånga (Kyrkbäkken, Skåne) BH (Bergström et al., 1997) and the Billegrav-2 BH in Bornholm (Kiipli et al., 2014b. Electron probe microanalysis (EPMA) data for the elements Fe, Mg, Mn, Ca, P, Ce, Cl, F and Y determined on apatite grain mounts from KKMB occurrences in Scandinavia were published by Sell and Samson (2011). These locations include Vollen, Arnestad (bulk sample), Mossen, Västergotland, Sweden (bulk sample) and Vasagård, Bornholm, Denmark (seven samples through sequence).

INTERPRETATION OF THE WIC APATITE GEOCHEMICAL DATA AND COMPARISON WITH THE KKMB AND OTHER BALTOSCANDIAN TEPHRA OF SANBIAN AGE

Elemental abundances in whole-rock MB samples can be ‘corrected’ using the formula of Kiipli et al. (2010, 2014a) to compensate for high Al values reflecting diagenetic processes, although this is not without its problems. We prefer instead to correlate MBs with potential source areas using igneous minerals unaffected by the super-eruption process, specifically zircon and apatite. Working in situ in thin section was preferred to mineral separation and mounting in epoxy, to preserve the petrographic relations and constraints of the crystals and thereby strengthen the geological interpretation of the acquired data.

Some of the LA-ICP-MS analyses from WIC apatite microphenocrysts exhibit a small amount of “contamination” from the matrix and/or inclusions. As great care was taken to analyze the center of each grain and avoid obvious inclusions, it is most likely that the laser has ablated through the grain into the matrix substrate. Al, concentrated in biotite and melt inclusions, is a useful indicator element for this problem, which in most cases is not significant in scale and mostly affects the content of the major elements Fe, Mn, and Mg. Al content is therefore used as a screening tool to recognize such analyses so that they can be excluded from diagrams (e.g., Figs. 10 and 11) where required. A further difference with the EPMA dataset is that data for F and Cl are lacking for the WIC and Baltoscandian MBs. While these halogens are extremely useful for discriminating and correlating MBs using EPMA-derived datasets (Emerson et al., 2004; Carey et al., 2009; Sell and Samson, 2011), these elements cannot be analyzed by LA-ICP-MS.

Five groups of igneous apatite microphenocrysts (Figs. 10 and S5) are recognized in the WIC apatite chemistry data, defined as groups CL1 and NC1–4. The most numerous analyses from the N Creake sample slides are largely euhedral grains defined as group NC1 (n = 29), of which a sub-group of seven grains (NC1m) display minor contamination from matrix or inclusions. N Creake samples contain three much rarer, subhedral-anhedral and geochemically distinct groups defined as NC2 (n = 4), NC3 (n = 1), and NC4 (n = 2). These groups are represented in both N Creake probe slides analyzed. The Claxby igneous apatite microphenocrysts comprise group CL1 (n = 15), of which six grains (sub-group CL1m) exhibit minor matrix contamination and are excluded from Figure 10. A further group of apatite grains (CL2, n = 6) are interpreted

© 2026 United Kingdom Research and Innovation.

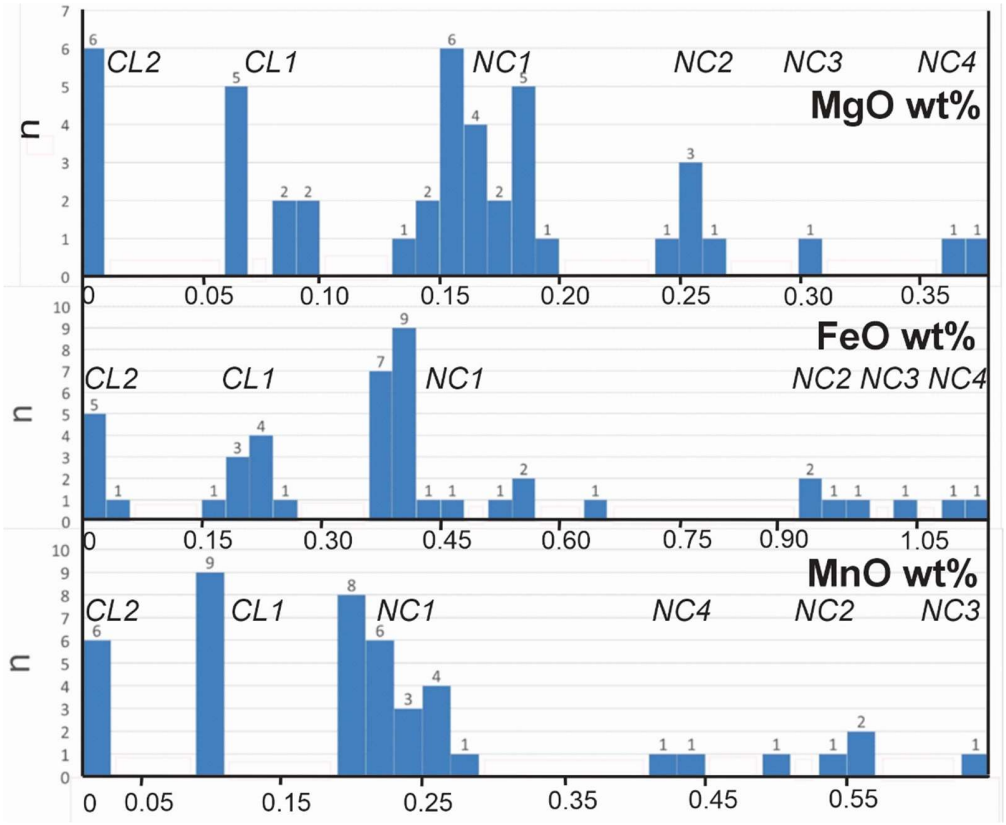

Figure 10. Histograms of MgO, FeO and MnO (wt%) concentrations in apatite grains from Wash Igneous Complex (WIC) samples analyzed by laser-ablation–inductively coupled plasma–mass spectrometry. Groups CL1 and CL2 are grains from Claxby 1 ~~BH~~ borehole samples. CL2 grains are authigenic and not plotted in other diagrams. Groups NC1–4 are apatite microphenocrysts from North Creake samples. Analyses from sub-groups CL1m and NC1m are "contaminated" by minor amounts of matrix or inclusions and are also not depicted on this diagram. The more numerous euhedral NC1 group may be associated with magma intrusion dated by chemical abrasion–isotope dilution–thermal ionization mass spectrometry at 453.70 ± 0.17 Ma possibly associated with caldera collapse. NC2–4 are rare abraded subhedral and anhedral apatite grains. NC3 is represented by a single apatite grain.

as authigenic. The latter grains are anhedral, exhibit a different cathodoluminescence color and a more patchy or sieve-like appearance (Fig. S5). They are derived from sites adjacent to the prominent quartz-carbonate-chlorite veining observed in probe slide E60870A and are inferred to be genetically-related to the development of these post-magmatic (and possibly much later) veins. The concentration of REE, MgO, FeO, and MnO in these grains is an order of magnitude lower than in the igneous grains (Fig. 10) and they show strong depletion of the LREE, as well as low Th and U concentrations. As these grains postdate the igneous history, which is the subject of this paper, they will not be considered further here, although they are included in the Supplemental Material dataset. The five igneous apatite microphenocryst groups are geochemically distinct, as shown by histogram plots for MgO, FeO, and MnO concentrations (Fig. 10).

Figure 11 comprises a set of bivariate trace and major element plots for geochemical data from igneous apatite microphenocrysts from the WIC and Baltoscandian MBs. We find that the ratio of Ce to Y, two elements that are widely represented in most apatite analytic datasets, and in themselves a powerful discriminant, represent a useful fractionation index on the abscissa of these plots. One minor drawback is that the compounded analytical (1σ) error of the Ce/Y ratio, exceeding 12% for the LA-ICP-MS data, and 17% for the EPMA analyses, is noticeably larger than for cross-plotted elements (Mg, Fe, and Mn). In general however, the analytical uncertainties using the EPMA and LA-ICP-MS methods are rather similar, judged on the analytical error data presented by Emerson et al. (2004) and the supplemental data published by Sell and Samson (2011) and Herrmann et al. (2021, 2023) and summarized in Table S4. Inset diagrams provide enlargements of those parts of the figures where the density of data complicates their interpretation. In addition, the EPMA data published by Sell and Samson (2011) for the KKMB at various Scandinavian localities are included. It is fortunate for our study that these authors sampled the Vasagård section on a stratigraphic basis, because it allows the geochemical differences between the main, lower part of the KKMB, and its thinner upper part, to be studied.

© 2026 United Kingdom Research and Innovation.

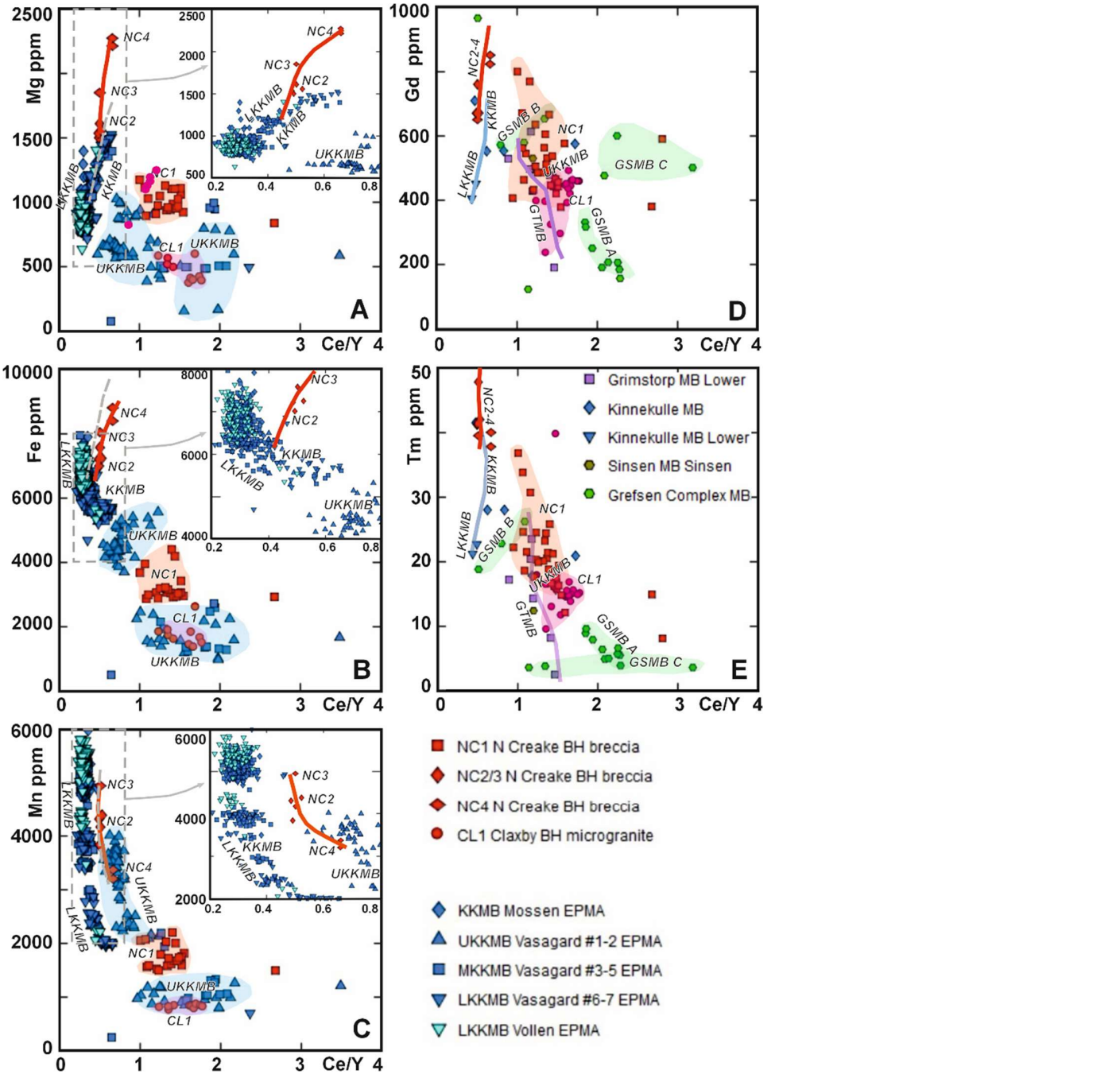

Figure 11. Bivariate plots for geochemical data from apatite microphenocrysts from Sandbian volcanic rocks. Left-hand side: apatites from five groups (NC1, NC2, NC3, NC4, CL1) recognized within Wash Igneous Complex (WIC) tuff-breccia and microgranite (laser-ablation–inductively coupled plasma–mass spectrometry [LA-ICP-MS] data; this work); and apatite grains from the Kinnekulle Metabentonite (KKMB) (electron probe microanalysis [EPMA] data; Sell and Samson, 2011). KKMB geochemistry data from these authors separated into: Lower KKMB (LKKMB), samples #3–7 from Vasagård section and the Vollen locality; Upper KKMB (UKKMB), samples #1–2 from Vasagård section; KKMB, uncategorized data from the Mossen locality. Authigenic grains (CL2) and contaminated grains (NC1m) from Wash Igneous Complex (WIC) are not plotted in Figs. 11A-C. Inset boxes are enlargements of parts of the figure where data density obscures the relationships. (A) MgO wt% vs. Ce/Y; (B) FeO wt% vs. Ce/Y; (C) MnO wt% vs. Ce/Y. Right-hand side: apatite microphenocryst compositional data from WIC tuff-breccia and microgranite (LA-ICP-MS data; this work) together with apatite bulk separates analyzed by ICP-MS (Batchelor, 2014). On these figures, individual components of metabentonite (MB) series and composite units are distinguished. (D) Gd vs. Ce/Y; (E) Tm vs. Ce/Y. GSMB A—Grefsen Group A; GSMB B—Grefsen Group B; GSMB C—Grefsen Group C; GTMB—Grimstorp MB; LKKMB—Lower Kinnekulle MB; UKKMB—Upper Kinnekulle MB; BH—borehole.

© 2026 United Kingdom Research and Innovation.

In Figure 11A, a bivariate plot of Mg versus Ce/Y, samples from the upper part (Sell and Samson (2011) samples #1 and #2) of the 0.75 m thick KKMB at Vasagård, here referred to as "Upper KKMB" (UKKMB) show a significant degree of scatter, with the separation of two main clusters greater than the 1σ compounded analytical uncertainty for the Ce/Y ratio; the lower five samples (#3–7) in the section (LKKMB) and analyses from the Mossen and Vollen bulk samples ("KKMB") form more distinct and relatively tight clusters along a linear trend. The presence of analyses from the bulk samples from the Vollen and Mossen localities in each of the LKKMB clusters gives confidence that the clusters are not an analytical artifact. Note that the division of the KKMB into two stratigraphic units in this way is not perfectly reflected by symbol separation in this diagram. This is because sample #1 of Sell and Samson (2011) likely contains some apatite grains reworked from the lower part of the MB, while sample #2 may be sampling across the intra-KKMB stratigraphic boundary.

The evidence presented in the previous paragraph supports the contention of several authors (e.g., Huff et al., 1992, 1996) that the KKMB is a composite product of at least two distinct super-eruptions, and that the UKKMB (Vasagård samples #1–2) is not preserved in some localities (e.g., Mossen). At Vollen, this is due to Caledonian thrusting and excision. At Mossen, the absence of UKKMB grains from the bulk sample may be due to contemporaneous erosion of the shallow carbonate platform, or it was not deposited.

The few WIC NC2–4 apatites identified occupy a linear trend (red line) parallel to, but not identical with that of the LKKMB, reflecting crystallization from more primitive (high Mg, NC4) to more evolved (lower Mg, NC2) melts. The projection of the melt trend beyond NC2 intersects the main cluster of LKKMB grains at its heart. Similar conclusions can be drawn from Figure 11B, the plot of Fe versus Ce/Y. Mn does not behave quite so coherently (Fig. 11C), with NC4 grains more comparable to one of the UKKMB clusters. More numerous CL1 grains occupy a tight cluster (possibly reflecting restricted compositional range in a short borehole core) adjacent to the two main clusters of UKKMB grains in all three diagrams (Figs. 11A–11C). While the UKKMB clusters are distinct at the level of the (1σ) analytical uncertainties identified earlier in this section, the cluster of CL1 grains could be identical to either KKMB cluster with the same uncertainties. Grains from the most numerous apatite group from N Creake, NC1, plot in an adjacent space to CL1 on the diagram in a less tight cluster lying between the main LKKMB and UKKMB clusters. Together, the CL1 and NC1 groups reflect a less coherent trend away from the strongly linear LKKMB trend and toward more evolved melts with lower content of Mg, Fe, and Mn (Figs. 11A–11C). If it is assumed that the matrix or inclusions inadvertently analyzed comprised/contained biotite, the FeO/MgO of such included material can be calculated. It is ~~c.~~~3.3 in the N Creake samples (sub-group NC1m), and ~~c.~~ ~2.5 in those from Claxby (sub-group CL1m).

In Figures 11D and 11E, the WIC apatite data are plotted together with the apatite separate data for the Arnestad Formation (including the KKMB) and Swedish correlatives published by Batchelor (2014b). The elements Gd and Tm were selected for plotting, but rather similar conclusions can be drawn when other REE are used. Three groups of apatite microphenocrysts are recognized in the Grefsen complex forming the lower part of the Arnestad Formation at Sinsen (Fig. 9). All three groups exhibit a negative Eu anomaly (Fig. 12) inferred to reflect fractionation of plagioclase from the melt prior to crystallization of apatite, but the amplitude of the anomaly varies between groups. The general increase of REE content within groups is attributed to fractionation of ferromagnesian minerals. Group A corresponds to the "primitive" group recognized by Batchelor (2014b) characterized by a relatively low content of REE (Fig. 12A).

The KKMB is also observed to form two distinct groups on Figures 11D and E, confirming the observation from Figures 11A and 11B. Samples NW45–47 (from Vollen), sample NW21 (from Sinsen), and sample SWB37 (from Billingen, near Mossen) form an elongated LKKMB cluster, lying on the same trend as the NC2–4 apatites from WIC; samples SWB31 (Billingen) and SWB97A-B (Fjåcka) plot away from the elongated LKKMB cluster at higher values of Ce/Y, and with greater similarity to CL1 and NC1, and are attributed to UKKMB. These relationships are also visible in Figure 12, the WIC NC2–4 apatites having REE patterns indistinguishable from those of the LKKMB group (Fig. 12D), while the patterns of the UKKMB group straddle the patterns of the CL1 apatites from the WIC Claxby Microgranite (Fig. 12E). Some of the microgranite patterns are enriched in LREE, which may reflect a greater degree of crustal contamination. The highest MBs in the Arnestad Formation (and Swedish correlatives) are attributed to the Grimstorp MBs (Fig. 9). The analyses from four localities published by Batchelor (2014b) define an elongated cluster colinear with the UKKMB and NC1 apatite group from WIC (Figs. 12D and 12E). They also intersect the Grefsen Group B cluster, suggesting a commonality of source. In Figure 12F, the chondrite-normalized patterns of the Lower Grimstorp MB (Bed #31 at Sinsen) and correlatives in Sweden straddle the patterns of WIC NC1 apatites. Overlying Bed #32 has a slightly divergent pattern with HREE depletion, comparable to Grefsen Group C (Fig. 12C), suggesting that the source of this tephra was likely not WIC.

© 2026 United Kingdom Research and Innovation.

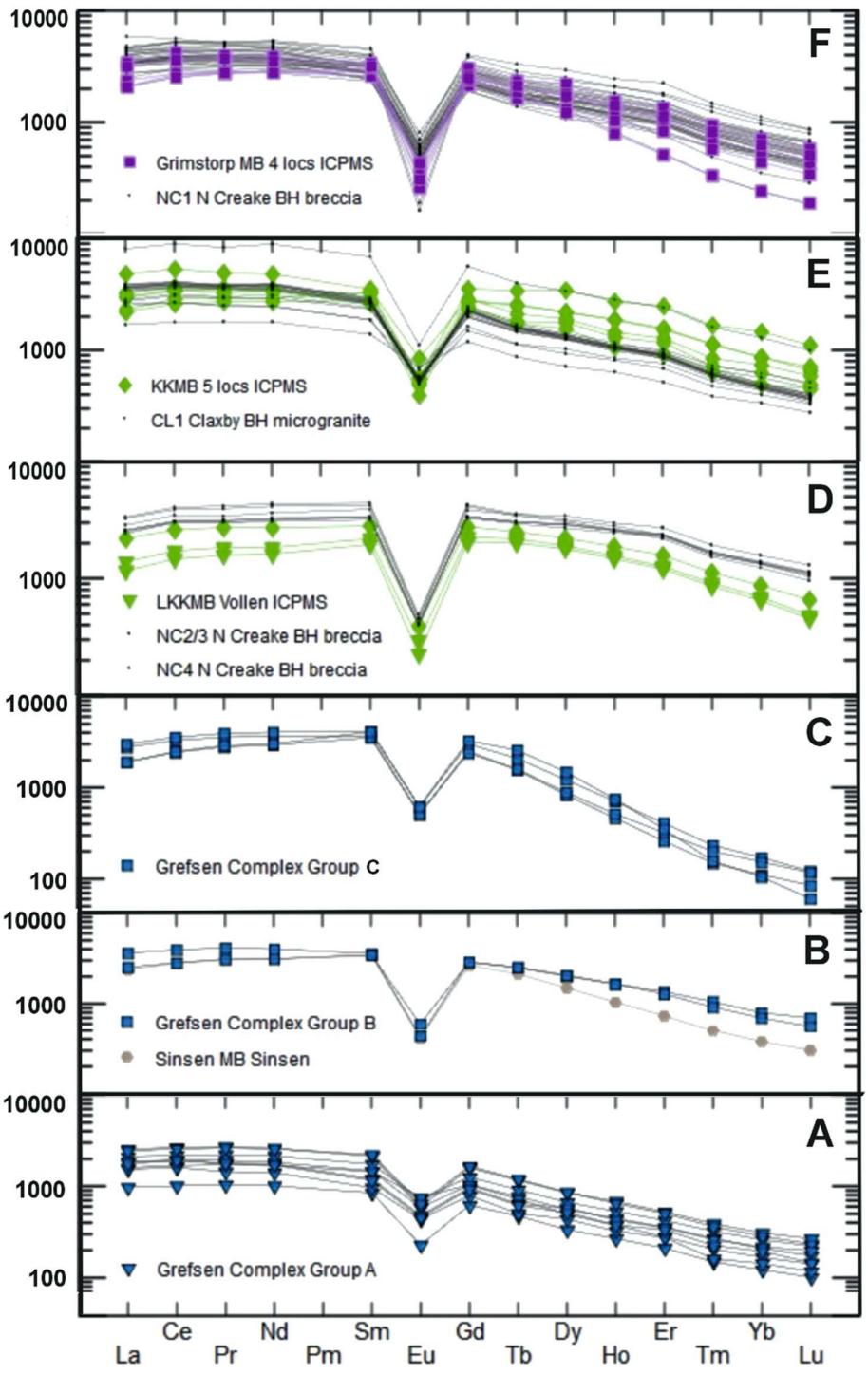

Figure 12. Chondrite-normalized (Sun and McDonough, 1989) rare earth element patterns for individual apatite microphenocrysts from Wash Igneous Complex (WIC) tuff-breccia and microgranite analyzed by laser-ablation–inductively coupled plasma–mass spectrometry (LA-ICP-MS; this work) and bulk apatite separates from the Arnestad Formation at Sinsen locality (and correlative Sularp and Skagen formations in Sweden) analyzed by ICP-MS (Batchelor, 2014b). (A) Grefsen Group A—"Primitive" Grefsen type of Batchelor (2014b), with a possible source in Snowdonia. (B) Grefsen Group B—part of "Evolved" Grefsen type of Batchelor (2014b), with a likely WIC source. (C) Grefsen Group C—another part of "Evolved" Grefsen type of Batchelor (2014b), with a possible Lake District source. (D) Group NC2–4 apatites from WIC with Vollen Lower Kinnekulle Metabentonite (LKKMB) samples. (E) Group CL1 apatites from WIC with KKMB from five localities. (F) Group NC1 apatites from WIC with Grimstorp MB apatites from four localities. BH—borehole.

© 2026 United Kingdom Research and Innovation.

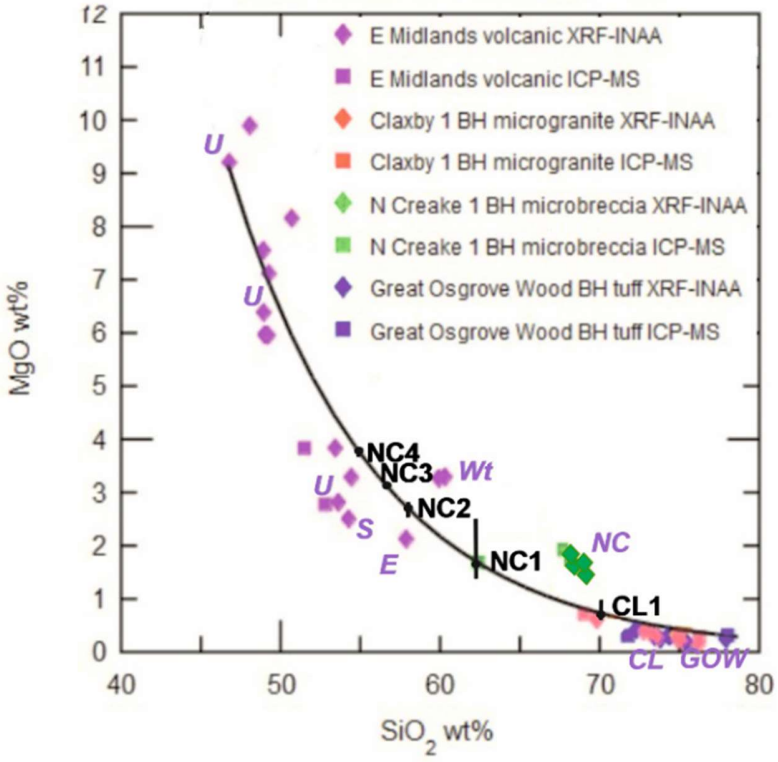

Figure 13. Model for magmatic evolution of melts in the Wash Igneous Complex (WIC) magmatic system. The regression line is a simple exponential fit to the whole-rock data to highlight a possible magmatic evolution indicated by the data. Legacy data (analytical procedures and published sources defined in caption to Fig. 6) are depicted with colored diamonds. New inductively coupled plasma–mass spectrometry (ICP-MS) whole-rock data are depicted with colored squares. Vertical bars indicate mean and range of MgO wt% calculated from laser ablation–ICP-MS data for each igneous apatite microphenocryst group in WIC, shown in bold font, following the precept of Prowatke and Klemme (2006). CL—Claxby 1; NC— North Creake 1; GOW—Great Osgrove Wood, XRF-INAA—Boreholes (BH) outside WIC shown in italic font: E—Eakring 146 BH; S—Sproxton BH; U—Upwood BH; Wt—Wittering and GSt2 BHs. Locations for these boreholes are shown on Figure 2 and simplified graphic logs in Figure 3. X-ray fluorescence–instrumental neutron activation analysis.

Elucidation of the factors controlling the geochemical grouping of apatite microphenocrysts in the WIC is achieved using the melt evolution model shown in Figure 13. Experimental work by Prowatke and Klemme (2006) has shown that the equilibrium melt/apatite ratio of Mg in many igneous rocks is ~10. Thus, it is possible to estimate to a first order the SiO_2 content of the melts in equilibrium with crystallizing apatite from the Mg contents of the apatites themselves. In Figure 13, a simple, exploratory exponential regression line has been fitted to the whole-rock data for the Claxby Microgranite, the Great Osgrove Wood rheomorphic tuff, and more primitive volcanic rocks sampled in boreholes in E England. The whole-rock data from the N Creake heterolithic tuff-breccia are excluded from this regression analysis, however, as they do not represent a melt composition. The mean MgO contents of the groups of apatite microphenocrysts (CL1, NC1–4), multiplied tenfold, have then been fitted onto the regression line, providing a first-order estimate of the SiO_2 contents of the coeval melts, assuming apatite crystallized in equilibrium with those melts. The mean MgO contents estimated for the melt in equilibrium with the apatites are shown by black dots, with vertical black lines showing the possible range of MgO values. The melt SiO_2 contents (and corresponding rock types) estimated from the model are as follows: NC4, 55% (basaltic andesite); NC3, 56% (andesite); NC2, 58% (andesite); NC1, 63% (dacite); and CL1, 70% (rhyodacite). For Claxby apatite group CL1, the estimated equilibrium SiO_2 content of the melt matches that for the rhyodacitic/rhyolitic composition of the host microgranite. We infer, therefore, that the apatites from Claxby samples crystallized in equilibrium with the microgranite magma, confirming the validity of the Prowatke and Klemme (2006) model. In contrast, the cluster of 10 whole-rock analyses for the N Creake tuff-breccia samples plots well away from the other groups of whole-rock data, highlighting a relatively more MgO-rich character. This likely reflects the incorporation of more mafic clasts in the heterolithic dacitic breccia (Fig. S1B). While apatites in group NC1 have MgO contents similar to the whole-rock samples,

© 2026 United Kingdom Research and Innovation.

and could have crystallized in equilibrium with precursor melt, groups NC2, NC3 and NC4 are significantly richer in MgO (Figs. 10 and 11A), suggesting that they are not in equilibrium with any melt fraction represented by the tuff-breccia. Thus, the presence of at least four distinct groups of igneous apatite microphenocrysts within each sample slide from N Creake indicates different magma sources, consistent with the chaotic, heterolithic nature of the tuff-breccia.

We conclude that source variability may have played a greater role in the evolution of the Arnestad MBs, particularly the Grefsen MB complex, than previously appreciated. Batchelor (2014b) preferred to explain the complexity he observed in the Grefsen MBs by invoking the generation of bimodal ("primitive" and "evolved") magmatic series from multi-cyclic evolution in a periodically replenished magma chamber, regarding this as a simpler explanation than one involving multiple sources. We will revisit this matter in the Discussion section. The chemical composition (of both apatite bulk samples and individual apatite grains) supports the correlation based on the new zircon TIMS U-Pb data, previously presented. These proposed correlations are summarized schematically in Figure 14, which includes speculations (from the thickness attributes of the correlated tephra) on the magnitude of eruptions associated with the events recorded by the U-Pb zircon ages.

A further interesting observation is that within the WIC apatites, the order of magmatic evolution from NC4 (judged most primitive in terms of Mg and Fe content) to NC2, NC1, and CL1 (most evolved) is not reflected in the REE patterns. This is possibly the same "decoupling" effect that influenced Batchelor (2014b) to name a group of Grefsen MB with relatively low REE content "primitive," when their high whole-rock content of Nb, Th, Y and Zr means they are actually quite evolved. Ordinarily increasing magmatic evolution, reflecting fractionation of ferromagnesian minerals followed by crustal contamination, should be reflected in increasing REE content. As this is not the observed situation here, we infer that the REE patterns are "snapshots" capturing different stages in the evolution of multiple batches of melt.

The following summarizes the interpretations of the apatite geochemical data made in the previous section.

- The KKMB is shown to be a composite tephra deposit as previously recognized by Sell and Samson (2011). The lower and middle parts of the KKMB, comprising perhaps 70%–80% of complete tephra profiles appear compositionally coherent in terms of Mg, Fe, and Mn content, suggesting formation in one eruptive event, likely postdating the phase of andesitic to dacitic magma evolution recorded by the NC4 to NC2 apatite microphenocryst evolutionary lineage. This is confirmed by the REE plots.
- The upper part of the KKMB (UKKMB) is less coherent in composition and may reflect a number of smaller eruptive events, although the similarity to Claxby CL1 apatites suggests that the same (WIC) source was involved. The diagram suggests that CL1 apatites may not have been erupted (and thus preserved in the tephra), although the CL1 apatites could be identical (within 1σ analytical uncertainty) to apatites in either of the surrounding UKKMB clusters
- The largest group of euhedral apatite microphenocrysts from N Creake, NC1, lie "on trend" between the main LKKMB, UKKMB, and Grimstorp Mg, Fe and, Mn compositional clusters, suggesting a genetic link.
- The wide range of content of Mg, Fe, and Mn in the LKKMB reflects the magnitude of the super-eruption which generated these tephra, which blasted most of the volcanic edifice "roots and all" into the atmosphere. By contrast, in the WIC, only individual components of the edifice, showing a restricted compositional ranges, were sampled by the boreholes studied.
- The REE bivariate plots also confirm the presence of three compositionally different groups within the Grefsen MB Complex, which may have different source regions. WIC may have been one of these.
- The lack of preservation of the UKKMB at several localities (e.g., Mossen) may result from a geographically variable footprint of tephra deposition due to atmospheric conditions, contemporaneous erosion subsequent to deposition and near the Caledonian orogenic front, tectonic excision.
- The presence of four geochemically distinct groups of igneous apatite microphenocrysts in the dacitic N Creake tuff-microbreccia, none of which is in equilibrium with a melt reflected in the whole-rock composition, highlights the strongly heterolithic nature of this lithology.

DISCUSSION

North Creake and Claxby BHs are located 65 km apart, both lying beyond the outer limits of the prominent negative gravity anomalies associated with the conjectured Wash Batholith (Chroston et al., 1987). This distance is toward the upper limit for caldera diameter and is associated with catastrophic mega-eruptions e.g., La Garita (Fish Canyon), Yellowstone, and Lake Toba (Lipman, 1999). While the N Creake tuff-breccia appears structurally related to the caldera or its walls, the melt which crystallized as the Claxby Microgranite, likely associated with post-eruptive caldera collapse, may not have been erupted and may have intruded beyond the caldera boundary. The crystallization ages of the zircons from Claxby and the older population of zircon grains from N Creake are identical within the analytical uncertainties and suggest some

© 2026 United Kingdom Research and Innovation.

underlying contemporaneous and shared magmatic process, such as the development of a long-lasting layer of crystal-rich mush zone (e.g., Cooper, 2017) beneath a nested caldera complex (Lipman, 1999). Caldera morphology is also indicated by the complexity of the gravity anomalies, though these are so far undrilled and their cause unproven. However, the available geophysical evidence points toward the presence of a complex granitic batholith underlying the volcanic components so far encountered. The term Wash Igneous Complex (WIC) is introduced here to incorporate all components of the silicic magmatic system, both volcanic and plutonic. A deep borehole to investigate the presently unexplored geothermal potential of this complex would provide further samples for study.

Various processes could have been involved in the formation of the N Creake heterolithic tuffaceous microbreccia. Lack of a fine-grained matrix apparently excludes origin as a lahar; lack of welding, excludes formation as a pyroclastic flow or "explosion breccia". The dacitic microbreccia contains clasts which are both more mafic and felsic than the host dacitic composition. Four distinct groups of apatite microphenocrysts (NC1–4) crystallized from andesitic-dacitic melt(s) and are not in equilibrium either with the dacitic whole-rock composition of the host, or the dacitic melt inclusions trapped in fractured quartz crystals (Fig. S3), also entrained in the microbreccia. These indicate that the latter is a strongly heterolithic rock type, likely originating as a "caldera collapse breccia" (Lipman, 1999). The latter, entraining admixed fragments of the caldera wall during collapse, are by far the most common type of breccia associated with caldera development (Lipman, 1999).

Although other interpretations are possible, we consider that the younger zircon population from N Creake is associated with magmatism and caldera collapse at 453.70 ± 0.55 Ma, which brought all the components of this heterolithic breccia together. The more numerous, euhedral NC1 apatite microphenocrysts are likely associated with this later magmatic activity. If so, it would explain the dissimilarity of NC1 apatite microphenocrysts to KKMB apatites. The best match for NC1 apatites are those from the overlying Grimstorp MB Bed #31 (Fig. 12F). The rare, abraded subhedral and anhedral grains of apatite groups NC4–2 are likely associated with earlier phases of andesitic-dacitic magmatism that led up to a catastrophic, ultraplinian super-eruption at ca. 454.4 Ma, recorded by the weighted mean ages for zircons from Claxby and the older zircon population in N Creake. This event generated the thicker, lower part of the KKMB. Confirmation of this hypothesis might require dating of zircon inclusions within apatites.

The CA-ID-TIMS data indicate the presence of possibly antecrystic zircon grains up to 456.68 ± 0.26 Ma in the Claxby sample. If the interpretation of the 453.7 ± 0.55 Ma age as associated with caldera collapse is correct, allowing for the analytical uncertainties, the WIC volcanic system existed for at least 3 m.y., possibly longer if WIC was also the source of slightly older antecrysts up to ca. 459 Ma in the Sinsen tephra (Ballo et al., 2019). This is compatible with the durations deduced for silicic magmatic systems of similar scale of Quaternary age in New Zealand (Wilson et al., 1995) and of Cenozoic age in the western United States (Lipman, 1999).

The discordancy of the LREE patterns between apatite groups NC2–4, CL1, and NC1 seen in Figure 12 likely reflects an increasing degree of crustal contamination in the melt of the more evolved, silicic compositions. Both whole-rock and apatite microphenocryst analyses from Claxby occupy a relatively tight cluster on geochemical plots, suggesting a limited range of melt composition, although this may reflect the limited core sample. Modeling indicates that the CL1 apatites are likely in equilibrium with the microgranitic host.

The rheomorphic tuffs from the Great Osgrove Wood BH are dissimilar to the samples from N Creake and Claxby BHs in terms of texture and whole-rock geochemical composition. The position of the short core immediately beneath the sub-Pennsylvanian unconformity means that major element composition (particularly K_2O) may have been affected by sub-unconformity weathering effects. Content of Nb, Y, and Zr, generally regarded as "immobile" under such conditions, is significantly higher than in the other WIC components and leads to a position closer to the slab-failure field in discrimination diagrams (Fig. 6). Whole-rock analyses show that Great Osgrove Wood rocks are more comparable to some of the evolved peralkaline rhyolites from Snowdonia, some 200 km distant. These characteristics suggest that if they are indeed associated with WIC, they may form a later, more evolved component of the complex, possibly post-dating development of the caldera system

The new CA-ID-TIMS zircon ages from WIC are identical within the 2σ uncertainties to TIMS zircon ages for the Lower and Upper Rhyolitic Tuff Formation of the Snowdon Volcanic Group of N Wales (Figs. 2 and 8), dated at 454.42–454.26 Ma (Lusty et al., 2017) and constrained by overlying marine mudstones of the *D. clingani* biozone (Longvillian sub-stage of the former British Caradoc Stage, now Katian; Molyneux et al., 2023). The Snowdon Volcanic Complex comprises calderas and intrusive granite bodies, which are an order of magnitude smaller, typically 5–6.5 km in diameter (Howells et al., 1991), than postulated here for the WIC. The sticky late-stage Snowdon magmas are highly evolved rhyolites and comendites enriched in incompatible elements such as Nb, Th, Y, and Zr (Leat et al., 1986; Howells et al.,1991). Similar

© 2026 United Kingdom Research and Innovation.

bimodal volcanic suites yielding within-plate geochemical signatures are found in backarc basins elsewhere in E Avalonia, e.g., in Wales (Bevins, 1982; Phillips et al., 2016 and in Ireland (McConnell et al., 1991).

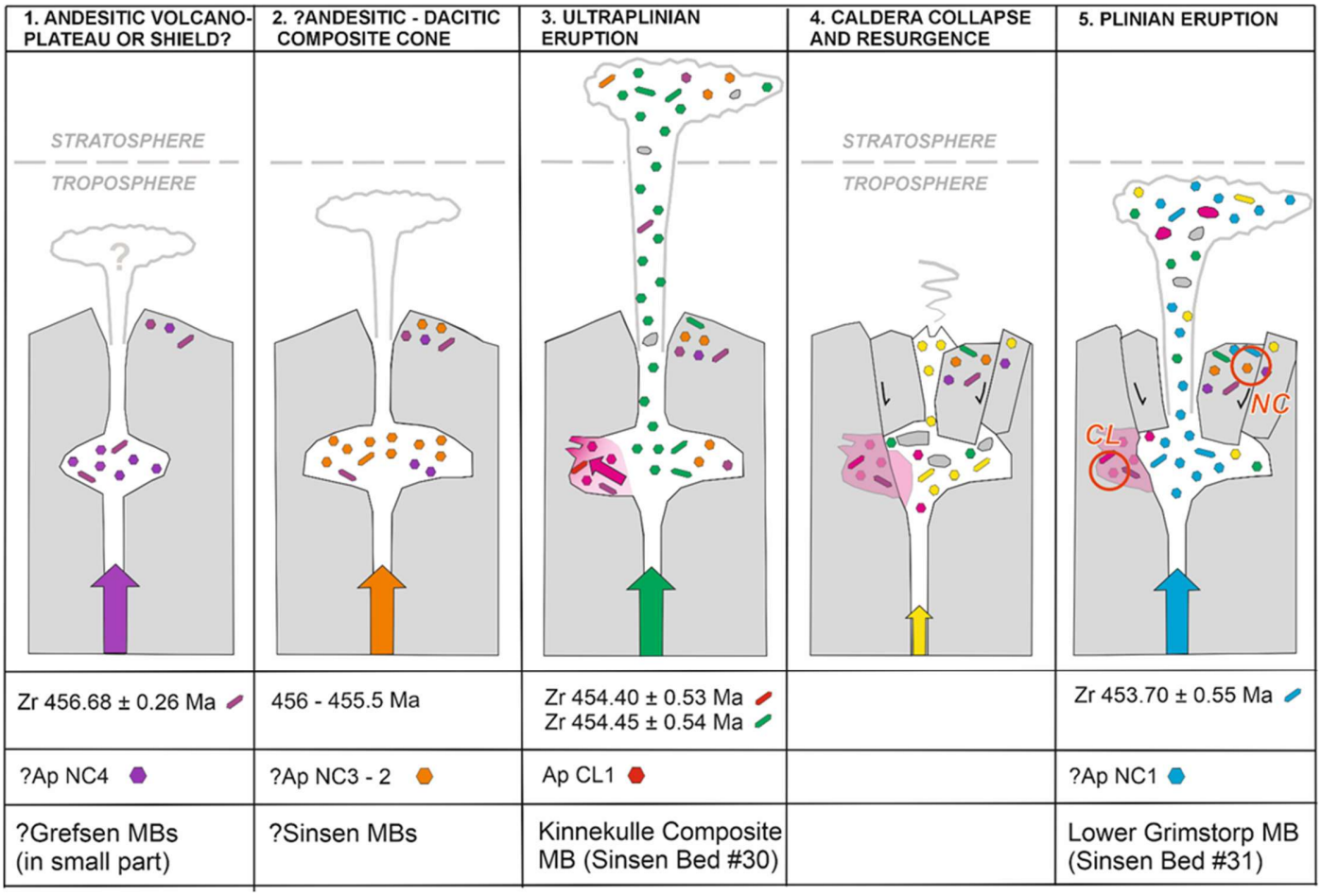

Figure 14. Schematic and conjectural illustration of Wash Igneous Complex (WIC) evolution constrained by thermal ionization mass spectrometry U-Pb zircon ages and igneous apatite microphenocryst chemistry. Speculation on the magnitude of eruption is based on the characteristics of possibly correlative Baltoscandian tephra. From ca. 457 Ma, pulses of mafic melt from a deep/base crustal reservoir undergo further maturation in an upper crustal magma chamber. WIC contributes to Baltoscandian tephra together with other possible sources in E Avalonia. Increasing crustal contamination of melt precedes a catastrophic ultraplinian eruption at ca. 454.4 Ma which generated the voluminous Kinnekulle tephra of Baltoscandia, in at least two phases. The second phase pf the Kinnekulle eruption may be associated with initial caldera collapse and injection of granite (Claxby Microgranite) into the caldera boundary. Following replenishment of the magma chamber, a Plinian eruption at ca. 453.7 Ma generated the earliest Grimstorp tephra. This was followed by further caldera collapse, which juxtaposed many older components of the caldera, to produce a heterolithic tuff-breccia (N Creake dacitic breccia). Subsequent evolution of a nested caldera complex may have involved eruption of a highly evolved tuff (Great Osgrove Wood rheomorphic tuff) and emplacement of an underpinning granite batholith (concealed Wash Batholith). MB—metabentonite; CL—location of rock sampled by the Claxby 1 BH; NC—location of rock sampled by the North Creake 1 BH.

There is insufficient space here to thoroughly review the extensive dataset of whole-rock geochemical data available for the Baltoscandian MBs particularly the KKMB; however, the following features are noteworthy. The division of the Grefsen MBs by Batchelor (2014b) into "primitive" and "enriched" types was on the basis of REE content. Other incompatible trace elements such as Nb, Th, Y, and Zr are significantly enriched in the "primitive" type, however, an apparent contradiction. We note that the elevated incompatible element content in this type (our Grefsen Group A) is comparable to that in evolved Group A2 lavas of the Snowdon Volcanic Group (Howells et al., 1991). We therefore suggest a Snowdonian source for Grefsen Group A, likely corresponding to Sinsen beds #7–14 in the section logged by Ballo et al. (2019); to the group of MBs at 93–95 m depth in the Billegrav-2 BH, Bornholm (Kiipli et al., 2014b); and possibly the analyses SWE153–154 at

© 2026 United Kingdom Research and Innovation.

4.5–5.0 m depth in the Röstånga BH, Skåne, published by Bergström et al. (1997). For Grefsen Group B, a WIC source is most likely and its signature reappears at various levels in the complex.

The new CA-ID-TIMS zircon ages indicate that the WIC is possibly older than the volcanic and plutonic components of the Borrowdale Volcanic Group (Lake District, N England; Fig. 2) dated by TIMS by Hughes et al. (1996) and Millward and Evans (2003). Because the latter data lie within the analytical uncertainty of the WIC data (Fig. 8), it is not possible to confirm that the WIC is older until higher precision data also become available for the Lake District. One distinctive feature of the Borrowdale volcanics is that several (but not all) andesitic and dacitic tuffs contain magmatic garnets (Fitton, 1972) that provide Sm-Nd isotopic ages of 457 ± 4 Ma (Thirlwall and Fitton, 1983). The garnets are considered to originate by contamination of the primary magma by aluminous material from pelitic strata deposited on the Mid-Ordovician deepwater extensional margin of E Avalonia following accretion of the Monian Terrane in Early Ordovician time (Schofield et al., 2008). In our view, the LD-EE Arc oversteps these earlier terrane boundaries. The distinctive HREE depletion exhibited by apatites of Grefsen Group C (samples NW13–17) might reflect a garnet residual source such as the Lake District, but this requires further investigation, particularly of apatite chemistry. The list of phenocrysts recorded from the Sandbian MBs in Baltoscandia includes amphibole, biotite, plagioclase, sanidine and quartz in addition to zircon and apatite (Haynes et al., 1995; Bergström et al., 1997; Kiipli et al., 2014a) but not garnet. There is no reason why garnet would not have survived transport and deposition in the Scandinavian MBs, when minerals with strong cleavage such as biotite and amphibole clearly did. Farther afield, other potential sources include the prolongation of the LD-EE Arc into Belgium, and the postulated volcanic arc associated with the Thor Suture on the Mid-North Sea High (Williamson et al., 2002).

The ratios of FeO/MgO in presumed matrix/inclusion biotite are compatible with the crystallization of biotite at relatively shallow crustal levels. They are also comparable with the FeO/MgO ratios observed in biotites from Baltoscandian MBs of Sandbian age, including the KKMB, examined by Haynes et al. (1995), Huff et al. (1996), Huff (2008), and Batchelor (2014b), but unlike those of Silurian MBs, which have FeO/MgO ratios typically in the range of 1–1.5 (Kiipli et al., 2014a). Haynes et al. (2011) note that Fe-rich biotites are typical of calderas developed within continental calc-alkaline arcs, such as Lake Toba and the Banda Arc in Indonesia and the Bishop Tuff and Long Valley Caldera of California.

The data presented here lead us to propose that at least some components of the Kinnekulle and Grimstorp tephras have their origins in the WIC. The very thick (up to 2 m) KKMB, long recognized as composite (Brusewitz, 1986; Huff et al., 1996; Huff, 2008; Sell and Samson, 2011; Batchelor, 2014b), may not preserve a full stratigraphy at all localities, as recognized by Sell and Samson (2011). At Vollen, the upper unit was tectonically excised during the Caledonian Orogeny. At the type locality near Mossen in Sweden, where UKKMB apatites appear to be absent from the bulk sample obtained by Sell and Samson (2011), it may have suffered penecontemporaneous erosion of the shallow-water carbonate platform. or may never have been deposited due to the vagaries of the footprint of tephra deposition. It is extremely fortunate that sampling of the 0.75-m-thick Vasagård section was carried out by Sell and Samson (2011) on a stratigraphic basis, although these authors do not specify the depth range of each sample precisely. WIC apatite groups NC4–2 exhibit a trend of andesitic to dacitic melt evolution which, if extrapolated, would intersect with the heart of the main cluster of analyses from the LKKMB. We infer that andesitic melt that was derived from a deep crustal mush zone evolved and interacted with more silicic material in upper crustal reservoirs, leading to the development of dacitic melt in a compositionally zoned magma chamber, catastrophically voided at ca. 454.4 Ma. The cause of the eruption is unknown but speculatively might have involved injection of a fresh pulse of melt from the lower crustal mush zone injected into sticky silicic magmas in the sub-volcanic magma chamber. The consequences, by contrast, are far clearer: an ultraplinian eruption column developed, injecting a vast volume of ash into the stratosphere, which was transported by westerly winds and subsequently deposited as a very thick tephra deposit across much of Baltoscandia. Following compaction, diagenesis, and lithification, this tephra became the lower part of the composite Kinnekulle Metabentonite. The contrasts in clustering pattern of the apatite chemical data on bivariate plots indicate a difference in eruptive style between the lower (main) and upper (less frequently preserved) divisions of the KKMB, confirming the composite structure of the bed described in the previous section and discussed earlier in this paragraph. It has been suggested that some of the ash may have been transported by SE trade winds, contributing to tephra in the Welsh Borderland, possibly crossing the Iapetus Ocean to reach the Southern Uplands of Scotland (Batchelor, 2014a), at that time a marginal part of the Laurentia palaeocontinent.

Integrating the interpretations mentioned previously, it is possible to propose a provisional (but non-unique) evolutionary model (Fig. 14) for the WIC magmatic system and its interaction with the late Sandbian stratigraphic record of Baltoscandia. The model contains speculative correlations between phases of crystallization of zircon and apatite microphenocrysts, and is severely constrained by the limited analytical dataset currently available. Following initiation of subduction at ca. 460 Ma, melts of basaltic and basaltic-andesite composition generated from the mantle-wedge overlying the subducting slab ponded at the base of the crust. Subsequent fractional crystallization of olivine, clinopyroxene, and plagioclase drove these

© 2026 United Kingdom Research and Innovation.

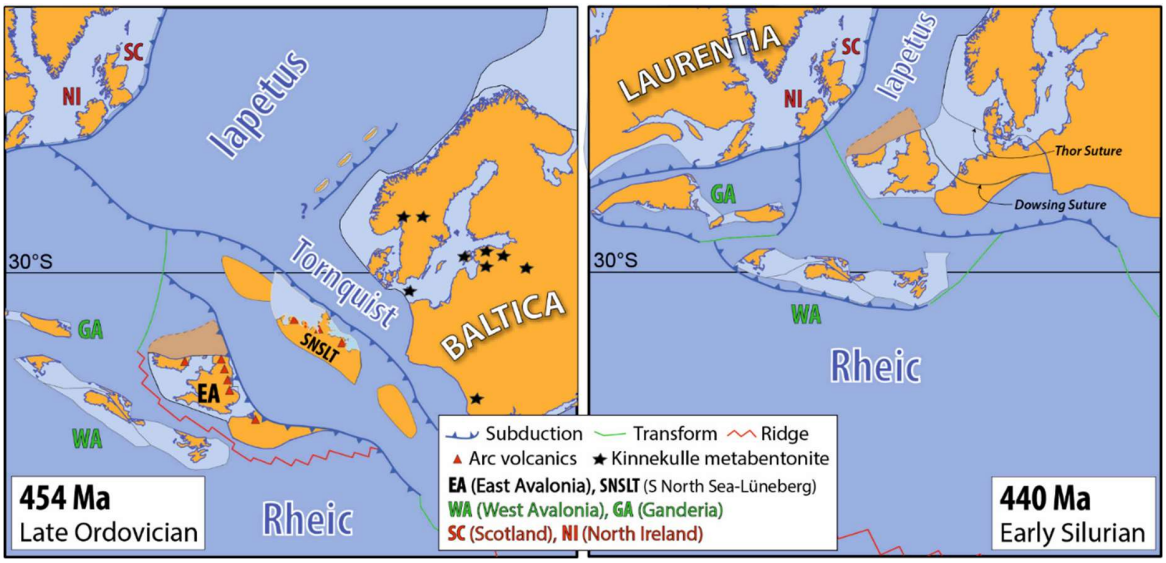

Figure 15. Paleogeographic reconstructions for Late Ordovician (ca. 454 Ma) and Early Silurian (ca. 440 Ma), after Torsvik and Cocks (2016) and Domeier (2016). Super-eruptions from arc volcanoes in England and backarc volcanoes in Wales and Ireland (Eastern Avalonia) deposited thick tephra of Sandbian age in Baltoscandia. A contribution from an inferred volcanic arc located on juvenile crust of the S North Sea Lüneberg Terrane, now concealed beneath the Mid-North Sea High (Fig. 1), cannot be excluded.

melts toward andesitic compositions, from which the earliest apatite microphenocrysts (NC4–2) crystallized. Increasing contamination by continental crust, likely in upper-crustal reservoirs, led to evolution of dacitic melts in upper crustal crystal-mush zones in an extensive (>65-km-wide) region underlying the developing volcanic province. This process was interrupted by a catastrophic ultraplinian eruption at 454.4 Ma, recorded by the LKKMB tephra in Baltoscandia. Quartz phenocrysts stable at depth suffered decompression during this event, or in a later phase of magmatism at 453.7 Ma, cracking and trapping the coexisting dacitic melt prior to marginal resorption at shallower depth. Beneath the source of the eruption, silicic magma bearing CL1 group apatites invaded the margins of the caldera, initiating the development of the underlying batholithic complex.. The progressive collapse of the caldera enabled episodic further eruption, but likely not of the same magnitude as the original super-eruption. The process of collapse allowed larger volumes of crust to enter the magma chamber and contaminate the melt. Many of the volcanic components—andesitic/dacitic clasts and derived, abraded NC4–2 group apatites, cracked quartz phenocrysts and silicic clasts bearing euhedral NC1 apatites—were incorporated into a caldera-collapse breccia during a less catastrophic magmatic event at ca. 453.7 Ma. This event is likely recorded by the earliest (Sinsen Bed #31) of the Grimstorp tephras in Scandinavia and was likely of Plinian magnitude. NC1 apatite grains could have crystallized from an associated magma or from an earlier melt batch. They do not appear to have crystallized from the progenitor melt to the LKKMB tephra, however.

Our data show good correspondence with the stratigraphic evolution of the Arnestad Formation in the Sinsen section in many aspects. There is more work to be done before our proposed correlation between the WIC source and (at least part of) the KKMB tephra can be regarded as proven. This would involve analysis of a far larger number of apatite microphenocrysts from other possible source(s), including Snowdonia, the Lake District, Ireland, and Belgium. Our analytical procedure would allow more detailed studies of slabbed borehole core through entire tephra sequences at various localities, particularly in Bornholm, where the succession appears most complete. It is interesting to note that the heterolithic N Creake breccia, normally a lithotype shunned by geochemists as a deviation from the path of melt evolution, has nevertheless yielded valuable insights into the latter process at WIC.

Key events in the closure of the Tornquist Sea have been described in more detail by Pharaoh (1999) and Torsvik and Rehnström (2003) and are depicted schematically in the paleogeographic maps and schematic lithospheric geotransect presented (Figs. 15 and 16). The WIC has been interpreted as a component of a calc-alkaline magmatic arc (Fig. 1) extending from N England (Pharaoh et al., 1993, 1995, 1997) to Belgium (André et al., 1986; Verniers et al., 2002) although the involvement of subduction is not universally accepted (Linnemann et al., 2012). Subduction of Tornquist ocean crust, likely part of a much larger Iapetus Ocean, was directed SW beneath Avalonia (upper plate) and not from the NW (Figs. 15 and 16), the vector advocated by most previous authors (e.g., Fitton and Hughes, 1970). It is likely that there was an oblique component to subduction ultimately resulting in slab failure. The time window for arc magmatism was from ca. 460 Ma

© 2026 United Kingdom Research and Innovation.

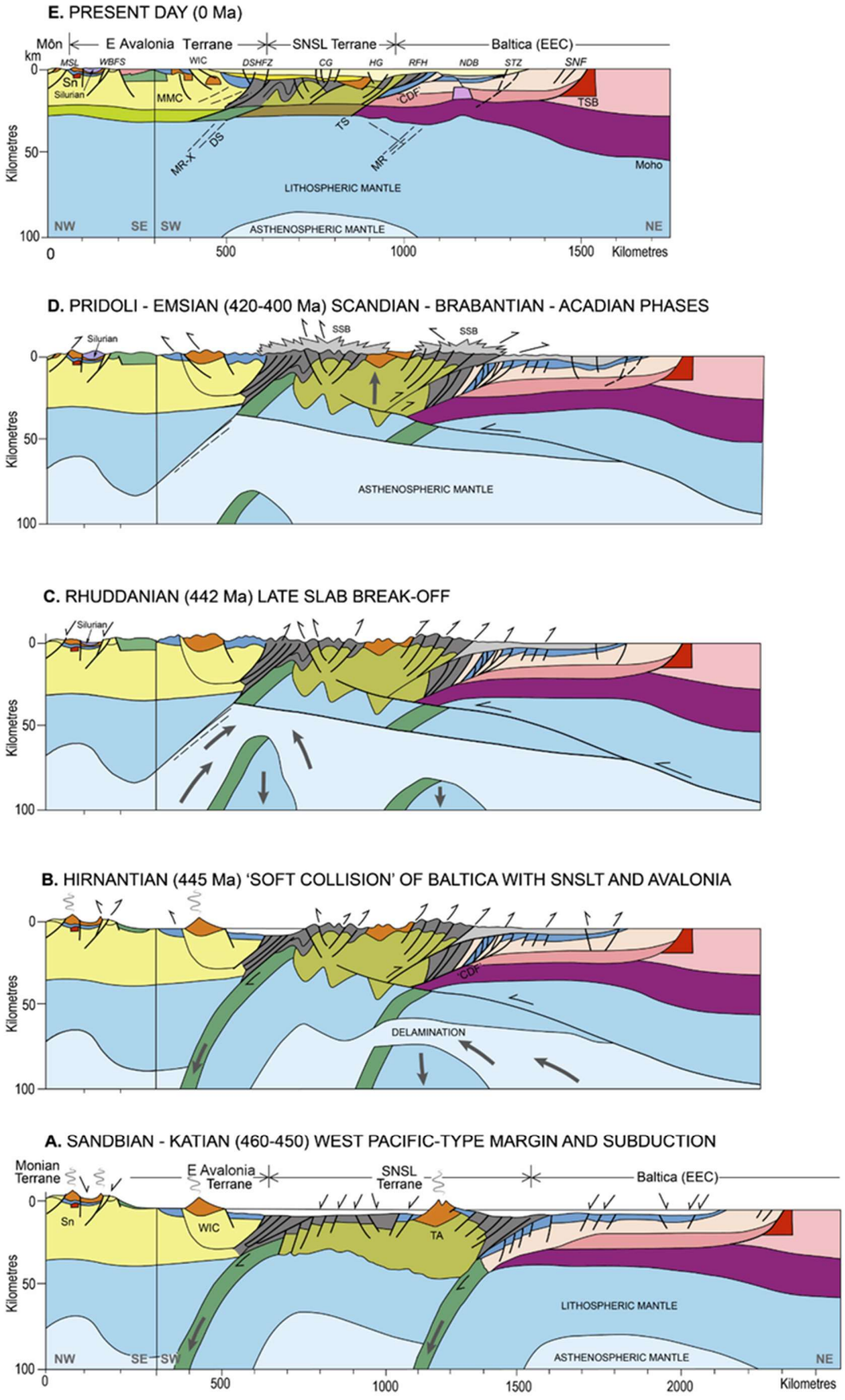

© 2026 UNITED KINGDOM RESEARCH AND INNOVATION.

Figure 16 (facing). Lithospheric profile to illustrate stages in the closure of the Tornquist Ocean Basin. Vertical scale grossly exaggerated.

(A) Sandbian-Katian (460–450 Ma). Closure of a West Pacific-margin type mosaic of small oceanic arc marginal basins intervening between Baltica and E Avalonia. High angle subduction beneath two volcanic arcs ("double subduction") leads to very rapid closure of the Tornquist Ocean by Late Ordovician time. The evidence for the western subduction zone (SZ) and arc is presented in this paper. The second postulated subduction system and the juvenile S North Sea Lüneberg Terrane (SNSLT) are nowhere exposed, lying concealed beneath the southern North Sea. These elements are postulated on the basis of geophysical and geometrical arguments (Pharaoh et al., 1995; Pharaoh, 1999; Williamson et al., 2002). Key: TA—Inferred Thor Arc; EEC—East European Craton; Sn—Snowdonia (Eryri).

(B) Hirnantian (445 Ma). "Soft collision" of Baltica and Eastern Avalonia results in deformation of the SNSLT and metamorphism of its clastic strata at greenschist to low amphibolite facies (Frost et al., 1981; Pharaoh, 1999), while basins on the extended margin of Baltica undergo inversion. These events are accompanied by slab failure, likely earliest at the easternmost SZ, and delamination of the sub-continental mantle. Subduction at the western SZ may have continued later, giving rise to late volcanic suites with alkalic tendencies in Snowdonia and the Lake District. 'CDF'—Caledonian Deformation Front.

(C) Rhuddanian (442 Ma). The injection of swarms of calc-alkaline lamprophyres of spessartitic affinity into the former backarc region of E Avalonia marks final slab failure, allowing access of asthenospheric mantle to shallower levels of the collisional system. The Thor (eastern) and Dowsing (western) crustal sutures develop at the locations of the former SZs.

(D) Pridoli-Emsian (420–400 Ma). Further shortening of the Tornquist collisional system results from the collision of Laurentia with Baltica, generating the Iapetus Suture Zone (Fig. 1), out of the plane of section of Figure 13, and subsequently, further Gondwana-derived microcontinents caught up in the Variscan Orogen. SSB—Inversion of Silurian successor deep-water basins.

(E) Present day. Modified from Williamson et al. (2002). Key to abbreviations, from west to east: MSL—Menai Strait Lineament; SN—Snowdonia (Eryri); WBFS—Welsh Borderland Fault System; MMC—Midland Microcraton; DS—Dowsing Suture; DSHFZ—Dowsing–S Hewett Fault Zone; CG—Central Graben; TS—Thor Suture; HG—Horn Graben; RFH—Ringköbing-Fyn High; 'CDF'—Caledonian Deformation Front; NDB—Norwegian-Danish Basin; STZ—Sorgenfrei-Tornquist Zone; SNF—Sveconorwegian Front; TSB—Trans-Scandinavian Batholith; MR—mantle reflectors identified on deep seismic reflection records. Note offset resulting from mantle delamination

(Darriwillian), on the basis of the onset of backarc volcanism in Wales (Kokelaar et al., 1984) and the oldest antecrysts from MBs in the Oslo Graben (Ballo et al., 2019), to ca. 442 Ma (earliest Silurian), the emplacement age (U-Pb: baddeleyite) of calc-alkaline, "within-plate" lamprophyres in the inferred backarc region (Noble et al., 1993). The latter, more enriched magmas with a deeper mantle source reflect slab detachment following "soft collision" (without granulite or eclogite facies metamorphism) between Baltica (lower plate) and the Gondwana-derived terranes, including Avalonia (upper plate).

In a "same-dip double-subduction" system analogous to the Recent Izu-Bonin-Marianas/ Ryukyu arc system of the West Pacific region (Holt et al., 2017), it might be possible to subduct an ocean basin a few thousand kilometers wide in the relatively short, permitted time window of 20–18 Ma. This would have resulted in a brief period of extremely violent ultraplinian mega-eruptions, setting up planet-wide impacts including cooling, glaciation, ^{13}C isotope excursions, and loss of biodiversity in the latest Ordovician (e.g., Buggisch et al., 2010).

As described in the Introduction, the inferred integrity of the LD-EE volcanic arc is put into question by the assertion of Waldron et al. (2025) that N England is transected by an Acadian (late Caledonian) suture, which they refer to as the Ynys Môn Line. Both conjectures invoke structures in the Caledonide basement, which are concealed by younger sedimentary basins, and there is insufficient space here to debate them exhaustively. If the LD-EE is a contiguous feature, overstepping earlier terrane boundaries associated with Early Ordovician accretion of the Monian (Ganderian?) Terrane (Schofield et al., 2008), the presence of a later suture is denied. If Waldron et al. (2025) are correct, the juxtaposition of the Borrowdale Volcanic Group in the Lake District block against the Wensleydale Batholith along the Dent Line (Fig. 2) is purely coincidental. In this case, existing models for the closure of the Iapetus and Tornquist oceans, and our understanding of the late Caledonian history of N England and the southern North Sea, would have to be reevaluated.

CONCLUSIONS

Analytical data from short cores from two boreholes near The Wash embayment in E England characterize volcanic and hypabyssal components of a Late Ordovician silicic magmatic system overlying a large, inferred granite batholith complex. The Wash Igneous Complex (WIC) formed part of a calc-alkaline magmatic arc extending from the Lake District to The Wash and possibly to Belgium (LD-EE Arc). New CA-ID-TIMS zircon ages of ca. 454.4 Ma (identical within 2σ analytical

© 2026 United Kingdom Research and Innovation.

uncertainties of <130 k.y.) for felsic samples from the N Creake and Claxby boreholes indicate contemporaneous igneous activity across the complex, although separated by some 65 km.

The new CA-ID-TIMS ages for the WIC are identical (within uncertainty) to precise CA-ID-TIMS zircon ages obtained for the Kinnekulle Metabentonite of Baltoscandia by Sell et al. (2013), Svensen et al. (2015) and Ballo et al. (2019), suggesting correlation. This is further supported by apatite microphenocryst geochemical data. However, the present lack of such data from other potential MB sources in the LD-EE Arc and its contemporaneous backarc region precludes stronger confirmation of the correlation until further isotopic and geochemical studies are completed. Thus, the WIC is presently regarded as a "candidate" source for components of the Kinnekulle and related tephra. Our preliminary findings suggest that the distinctive signature of highly evolved peralkaline magmas from Snowdonia may be recorded in some tephra of the slightly older Grefsen MB complex, interbedded with tephra sourced from WIC and other possible sources in E Avalonia.

North Creake BH drilled an unwelded tuffaceous microbreccia that contains intermediate clasts, cracked quartz phenocrysts with dacitic melt inclusions, and felsic blocks. Such components are representative of the walls of large felsic caldera systems associated with mega-eruptions, for example, in the western United States (Lipman, 1999) and the Taupo Zone of New Zealand (Wilson et al., 1995). Both of the samples analyzed, separated by a vertical distance of 23 m, contain rare non-euhedral, abraded, rounded, and broken apatite microphenocrysts (groups NC4–2) not represented in the KKMB tephra of Scandinavia. These grains, likely derived from more primitive andesitic melts, exhibit a trend in magmatic evolution ending in the source of the major (lower) part of the KKMB. A cluster of Claxby CL1 apatite analyses most closely resemble those in the less widely distributed upper part of the composite KKMB.. The host melt formed a post-eruption granite flood of the roots of the caldera. N Creake breccia is dominated by euhedral NC1 apatites most comparable to apatites in the Grimstorp MB overlying the KKMB. The CA-ID-TIMS age of the younger zircon population in N Creake, 453.70 ± 0.17 Ma, may date a Plinian eruption associated with caldera-collapse and formation of the Grimstorp tephra., Our studies confirm the potential of both high-precision CA-ID-TIMS U-Pb age determination of zircon and apatite microphenocryst geochemistry in the correlation of ancient super-eruptive sources and their associated tephra (e.g., Sell and Samson, 2011; Sell et al., 2013). These grains have survived the vagaries of a violent ultraplinian mega-eruption column, stratospheric transport, depositional and diagenetic processes, and in the case of the inferred sources, hydrothermal and regional greenschist metamorphism, apparently unscathed. They help to elucidate potential sources in ancient volcanic complexes and, at the same time, to unravel the stratigraphic complexities of composite MB beds, which may be more common than previously assumed. Detailed stratigraphically controlled studies using serial probe slides analyzed by LA-ICP-MS have the capability to discriminate individual phases of eruption and to recognize missing tephra stratigraphic section. Such studies offer the potential for realistic assessments to be made of the magnitude and number of super-eruptive events involved in the accumulation of these thick tephra as originally envisaged by Huff et al. (1992, 1996) and Bergström et al. (1995). In addition, data from such studies have the potential to identify and correlate sources of ancient tephra deposits.

ACKNOWLEDGMENTS

This work was supported by grant 2534.0422 from the Natural Environment Research Council (NERC) National Environmental Isotope Facility (NEIF). Nigel Woodcock and Sedgwick Museum, Department of Geology, Cambridge University, are thanked for provision of the North Creake BH core samples. The Manager of the Heidelberg Materials cement works at Skövde, Sweden is thanked for quarry access. John Fletcher created excellent thick probe slides from very difficult materials. The late Richard Batchelor, of St Andrews University, provided apatite separates; both he and Richard Merriman inspired our interest in metabentonites; Michael Carr developed the IgPet diagram plotting software; Pieter Vermeesch made available the IsoplotR software; and Liz Scott and Jim Rayner assisted with the diagrams. We thank Steve Noble and Holly Unwin for helpful comments and the journal referees, Scott Samson and Cees van Staal, for their detailed reviews. Pharaoh thanks the many participants of the European Science Foundation–supported EUROPROBE Programme (1993–2002) and associated PACE TMR (Palaeozoic Amalgamation of Central Europe Training and Mobility of Researchers) Network supported by the European Union, who shaped his views on the topics addressed here. The inspirational leadership of this programme by the late David Gee of Uppsala University is recognized here. Torsvik acknowledges financial support by the Research Council of Norway through its Centers of Excellence Scheme, project number 332523 (PHAB). This paper is published with the approval of the Executive Director, British Geological Survey (UKRI).

REFERENCES CITED

André, L., Hertogen, J., and Deutsch, S., 1986, Ordovician-Silurian magmatic provinces in Belgium and the Caledonian orogeny in middle Europe: Geology, v. 14, p. 879–882, https://doi.org/10.1130/0091-7613(1986)14<879:OMPIBA>2.0.CO;2.

Armstrong, H.A., 2007, On the cause of the Ordovician glaciation, *in* Williams, M., Haywood, A.M., Gregory, F.J., and Schmidt, D.N., eds., Deep Time Perspectives on Climate Change: Marrying the Signal from Computer Models and Biological Proxies: Geological Society, London, Micropalaeontological Society Special Publication, v. 2, p. 101–121, https://doi.org/10.1144/TMS002.5.

© 2026 United Kingdom Research and Innovation.

Ballo, E.G., Augland, L.E., Hammer, Ø., and Svensen, H.H., 2019, A new age model for the Ordovician (Sandbian) K-bentonites in Oslo, Norway: Palaeogeography, Palaeoclimatology, Palaeoecology, v. 520, p. 203–213, https://doi.org/10.1016/j.palaeo.2019.01.016.

Batchelor, R.A., 2014a, Metabentonites from the Sandbian Stage, Upper Ordovician, in Scotland—A geochemical comparison with their equivalents in Baltoscandia: Scottish Journal of Geology, v. 50, p. 159–163, https://doi.org/10.1144/sjg2014-004.

Batchelor, R.A., 2014b, Geochemistry of Upper Ordovician metabentonites and their cognate apatite microphenocrysts from Norway and Sweden: Geologiska Föreningens i Stockholm Förhandlingar, v. 136, p. 387–397, https://doi.org/10.1080/11035897.2013.854272.

Bauert, H., lsozaki, Y., Holmer, L.E., Aoki, K., Sakata, S., and Hirata, T., 2014, New U-Pb zircon ages of the Sandbian (Upper Ordovician) "Big K-bentonite" in Baltoscandia (Estonia and Sweden) by LA-ICPMS: Geologiska Föreningens i Stockholm Förhandlingar, v. 136, p. 30–33, https://doi.org/10.1080/11035897.2013.862854.

Bergström, S.M., Huff, W.D., Kolata, D.R., and Bauert, H., 1995, Nomenclature, stratigraphy, chemical fingerprinting, and areal distribution of some Middle Ordovician K-bentonites in Baltoscandia: Geologiska Föreningens i Stockholm Förhandlingar, v. 117, p. 1–13, https://doi.org/10.1080/11035899509546191.

Bergström, S.M., Huff, W.D., Kolata, D.R., Yost, D.A., and Hart, C.,1997, A unique Middle Ordovician K-bentonite bed succession at Röstånga, S Sweden: Geologiska Föreningens i Stockholm Förhandlingar, v. 119, p. 231–244, https://doi.org/10.1080/11035899509546191.

Bergström, S.M., Schmitz, B., Saltzmann, M.R., and Huff, W.D., 2010, The Upper Ordovician Guttenberg $\delta^{13}C$ excursion (GICE) in North America and Baltoscandia. Occurrence, chronostratigraphic significance and paleoenvironmental relationships, *in* Finney, S.C., and Berry, W.B.N., The Ordovician Earth System: Geological Society of America Special Paper 466, p. 7–67, https://doi.org/10.1130/2010.2466(04).

Bergström, S.M., Eriksson, M.E., Schmitz, B., Young, S.A., and Ahlberg, P., 2016, Upper Ordovician $\delta^{13}C_{org}$ chemostratigraphy, K-bentonite stratigraphy, and biostratigraphy in southern Scandinavia: A reappraisal: Palaeogeography, Palaeoclimatology, Palaeoecology, v. 454, p. 175–188, https://doi.org/10.1016/j.palaeo.2016.04.037.

Berthelsen, A., 1998, The Tornquist Zone northwest of the Carpathians: An intraplate pseudosuture: Geologiska Föreningens i Stockholm Förhandlingar, v. 120, p. 223–230, https://doi.org/10.1080/11035899801202223.

Bevins, R.E., 1982, Petrology and geochemistry of the Fishguard Volcanic Complex, Wales: Geological Journal, v. 17, p. 1–21, https://doi.org/10.1002/gj.3350170102.

Bott, M.H.P., Robinson, P., and Kohnstamm, M.A., 1978, A granite beneath Market Weighton, east Yorkshire: Journal of the Geological Society, v. 135, p. 535–543, https://doi.org/10.1144/gsjgs.135.5.0535.

Brusewitz, A.M., 1986, Chemical and physical properties of Palaeozoic potassium bentonites from Kinnekulle, Sweden: Clays and Clay Minerals, v. 34, p. 442–454, https://doi.org/10.1346/CCMN.1986.0340411.

Buggisch, W., Joachimski, M.M., Lehnert, O., Bergström, S.M., Repetski, J.E., and Webers, G.F., 2010, Did intense volcanism trigger the first Late Ordovician icehouse?: Geology, v. 38, p. 327–330, https://doi.org/10.1130/G30577.1.

Busby, J.P., Walker, A.S.D., and Rollin, K.E., 2006, Regional Geophysics of South-east England: Keyworth, Nottingham, UK, British Geological Survey, Version 1.0 on CD-ROM.

Carey, A., Samson, S.D., and Sell, B., 2009, Utility and limitations of apatite phenocryst chemistry for continent-scale correlation of Ordovician K-bentonites: The Journal of Geology, v. 117, p. 1–14, https://doi.org/10.1086/594368.

Chroston, P.N., Allsop, J.M., and Cornwell, J.D., 1987, New seismic refraction evidence on the origin of the Bouguer anomaly low near Hunstanton. Norfolk: Proceedings of the Yorkshire Geological Society, v. 46, p. 311–319, https://doi.org/10.1144/pygs.46.4.311.

Cocks, L.R.M., and Fortey, R.A., 1982, Faunal evidence for oceanic separations in the Palaeozoic of Britain: Journal of the Geological Society, v. 139, p. 465–478, https://doi.org/10.1144/gsjgs.139.4.0465.

Cocks, L.R.M., and Fortey, R.A., 2009, Avalonia: a long-lived terrane in the Lower Palaeozoic?, *in* Bassett, M.G., ed., Early Palaeozoic Peri-Gondwana Terranes: Geological Society, London, Special Publication 325, p. 141–155, https://doi.org/10.1144/SP325.7.

Cohen, K.M., Finney, B.C., Gibbard, P.L., and Fen, J.-K., 2013, ICS International Chronostratigraphic Chart: Episodes, v. 36, p. 199–204, https://doi.org/10.18814/epiiugs/2013/v36i3/002.

Compston, W., 2000, Interpretations of SHRIMP and isotope dilution zircon ages for the geological time-scale: 1. The early Ordovician and late Cambrian: Mineralogical Magazine, v. 64, p. 43–57.

Compston, W., and Gallagher, K., 2012, New SHRIMP zircon ages from tuffs within the British Palaeozoic stratotypes: Gondwana Research, v. 21, p. 719-727,

Condon, D.J., Schoene, B., McLean, N.M., Bowring, S.A., and Parrish, R.R., 2015, Metrology and traceability of U-Pb isotope dilution geochronology (EARTHTIME Tracer Calibration Part I): Geochimica et Cosmochimica Acta, v. 164, p. 464–480, https://doi.org/10.1016/j.gca.2015.05.026.

Cooper, K.M., 2017, What does a magma reservoir look like? The "Crystal's Eye" view: Elements, v. 13, p. 23–28, https://doi.org/10.2113/gselements.13.1.23.

Cornwell, J.D., and Walker, A.D., 1989, Regional geophysics, *in* Plant, J.A., and Jones, D.G., eds., Metallogenic Models and Exploration Criteria for Buried Carbonate-Hosted Ore Deposits—A Multidisciplinary Study in Eastern England: Keyworth, Nottingham, UK, British Geological Survey, and London, The Institution of Mining and Metallurgy, p. 25–52.

Crowder, E., Rawlinson, N., Cornwell, D.G., Sammarco, C., Galetti, E., and Curtis, A., 2021, New insights into North Sea deep crustal structure and extension from transdimensional ambient noise tomography: Geophysical Journal International, v. 224, p. 1197–1210, https://doi.org/10.1093/gji/ggaa475.

Domeier, M., 2016, A tectonic scenario for the Iapetus and Rheic Oceans: Gondwana Research, v. 36, p. 275–295, https://doi.org/10.1016/j.gr.2015.08.003.

Dunham, K.C., 1974, Granite beneath the Pennines in North Yorkshire: Proceedings of the Yorkshire Geological Society, v. 40, p. 191–194, https://doi.org/10.1144/pygs.40.2.191.

Emerson, N.R., Simo, J.A., Byers, C.W., and Fournelle, J., 2004, Correlation of (Ordovician, Mohawkian) K-bentonites in the upper Mississippi valley using apatite chemistry: implications for stratigraphic interpretation of the mixed carbonate-siliciclastic Decorah Formation: Palaeogeography, Palaeoclimatology, Palaeoecology, v. 210, p. 215–233, https://doi.org/10.1016/j.palaeo.2004.02.042.

© 2026 United Kingdom Research and Innovation.

Evans, J.A., Millar, I.L., and Noble, S.R., 1995, Hydration during uplift is recorded by reset Rb-Sr whole-rock ages: Journal of the Geological Society, v. 152, p. 209–212, https://doi.org/10.1144/gsjgs.152.2.0209.
Fitton, J.G., 1972, The genetic significance of almandine-pyrope phenocrysts in the calc-alkaline Borrowdale Volcanic Group, Northern England: Contributions to Mineralogy and Petrology, v. 36, p. 231–248, https://doi.org/10.1007/BF00371434.
Fitton, J.G., and Hughes, D.J., 1970, Volcanism and plate tectonics in the British Ordovician: Earth and Planetary Science Letters, v. 8, p. 223–228, https://doi.org/10.1016/0012-821X(70)90180-9.
Franke, D., 1995, ~~The~~ Caledonian terranes along the southwestern border of the East European platform—Evidence, speculation and open questions~~,~~ Studia Geophysica et Geodaetica, v. 39, p. 241–256, https://doi.org/10.1007/BF02295815.
Fritschle, T., Daly, J.S., McConnell, B., Whitehouse, M.J., Menuge, J.F., Buhre, S., Mertz-Kraus, R., and Döpke, D., 2018, Peri-Gondwanan Ordovician arc magmatism in southeastern Ireland and the Isle of Man: Constraints on the timing of Caledonian deformation in Ganderia: Geological Society of America Bulletin, v. 130, p. 1918–1939, https://doi.org/10.1130/B31949.1.
Frost, R.T.C., Fitch, F.J., and Miller, J.A., 1981, The age and nature of the crystalline basement of the North Sea Basin, *in* Illing, I.V. and Hobson, G.D., eds., Petroleum Geology of the Continental Shelf of North West Europe: London, Institute of Petroleum, p. 43–57.
Gill, J.B., 1981, Orogenic Andesites and Plate Tectonics: Berlin, Springer, 392 p., https://doi.org/10.1007/978-3-642-68012-0.
Haynes, J.T., Melson, W.G., and Kunk, M.J., 1995, Composition of biotite phenocrysts in Ordovician tephras casts doubt on the proposed trans-Atlantic correlation of the Millbrig K-bentonite (United States) and the Kinnekulle K-bentonite (Sweden): Geology, v. 23, p. 847–850, https://doi.org/10.1130/0091-7613(1995)023<0847:COBPIO>2.3.CO;2.
Haynes, J.T., Huff, W.D., and Melson, W.G., 2011, Major Ordovician tephras generated by caldera forming explosive volcanism on continental crust: Evidence from biotite compositions, *in* Gutiérrez-Marco, J.C., Rábano, J., and Garcia-Bellido, D., eds., Ordovician of the World: Madrid, Cuadernos del Museo Geominero, Instituto Geológica y Minero de España, v. 14, p. 229–235.
Herrmann, A.D., Haynes, J.T., Robinet, R.M., and Emerson, N.R., 2021, Machine learning applied to K-bentonite geochemistry for identification and correlation: The Ordovician Hagan K-bentonite complex case study: Geosciences, v. 11, 380, https://doi.org/10.3390/geosciences11090380.
Herrmann, A.D., Haynes, J.T., and Robinet, R.M., 2023, Testing tectonostratigraphic hypotheses of the Blountian phase of the Taconic Orogeny in the southern Appalachians through an integrated geochronological and sedimentological study of Ordovician K-bentonites and quartz arenites: Minerals (Basel), v. 13, 807, https://doi.org/10.3390/min13060807.
Hofmann, A.W., 1988, Chemical differentiation of the Earth: The relationship between mantle, continental crust and oceanic crust: Earth and Planetary Science Letters, v. 90, p. 297–314, https://doi.org/10.1016/0012-821X(88)90132-X.
Holt, A.F., Royden, L.H., and Becker, T.W., 2017, The dynamics of double subduction: Geophysical Journal International, v. 209, p. 250–265, https://doi.org/10.1093/gji/ggw496.
Howells, M.F., Reedman, A.J., and Campbell, S.D.G., 1991, Ordovician (Caradoc) Marginal Basin Volcanism in Snowdonia (North-West Wales): London, HMSO for the British Geological Survey, 191 p.
Huff, W.D., 2008, Ordovician K-bentonites: Issues in interpreting and correlating ancient tephras: Quaternary International, v. 178, p. 276–287, https://doi.org/10.1016/j.quaint.2007.04.007.
Huff, W.D., Bergström, S.M., and Kolata, D.R., 1992, Gigantic Ordovician volcanic ash fall in North America and Europe: Biological, tectonomagmatic, and event-stratigraphic significance: Geology, v. 20, p. 875–878, https://doi.org/10.1130/0091-7613(1992)020<0875:GOVAFI>2.3.CO;2.
Huff, W.D., Kolata, D.R., Bergström, S.M., and Zhang, Y.S., 1996, Large-magnitude Middle Ordovician volcanic ash falls in North America and Europe: Dimensions, emplacement and post-emplacement characteristics: Journal of Volcanology and Geothermal Research, v. 73, p. 285–301, https://doi.org/10.1016/0377-0273(96)00025-X.
Hughes, R.A., Evans, J.A., Noble, S.R., and Rundle, C.C., 1996, U-Pb chronology of the Ennerdale and Eskdale intrusions supports sub-volcanic relationships with the Borrowdale Volcanic Group (Ordovician, English Lake District): Journal of the Geological Society, v. 153, p. 33–38, https://doi.org/10.1144/gsjgs.153.1.0033.
Irvine, T.N., and Baragar, W.R.A., 1971, A guide to the chemical classification of the common volcanic rocks: Canadian Journal of Earth Sciences, v. 8, p. 523–548, https://doi.org/10.1139/e71-055.
Jaffey, A.H., Flynn, K.F., Glendeni, L.E., Bentley, W.C., and Essling, A.M., 1971, Precision measurement of half-lives and specific activities of ^{235}U and ^{238}U: Physical Review C, v. 4, p. 1889–1906, https://doi.org/10.1103/PhysRevC.4.1889.
Kearey, P., and Rabae, A.M., 1996, Relic subduction in the southern North Sea recognized from deep seismic reflection and gravity data: Tectonophysics, v. 258, p. 115–124, https://doi.org/10.1016/0040-1951(95)00189-1.
Kiipli, T., Kallaste, T., and Nestor, V., 2010, Composition and correlation of volcanic ash beds of Silurian age from the eastern Baltic: Geological Magazine, v. 147, p. 895–909, https://doi.org/10.1017/S0016756810000294.
Kiipli, T., Soesoo, A., and Kallaste, T., 2014a, Geochemical evolution of Caledonian volcanism recorded in the sedimentary rocks of the eastern Baltic region, *in* Corfu, F., Gasser, D., and Chew, D.M., eds., New Perspectives on the Caledonides of Scandinavia and Related Areas. Geological Society, London, Special Publication 390, p. 177–192, https://doi.org/10.1144/SP390.5.
Kiipli, T., Kallaste, T., Nielsen, A.T., Schovsbo, N.H., and Siir, S., 2014b, Geochemical discrimination of the Upper Ordovician Kinnekulle Bentonite in the Billegrav-2 drill core section, Bornholm, Denmark: Estonian Journal of Earth Sciences, v. 63, p. 264–270, https://doi.org/10.3176/earth.2014.29.
Kokelaar, B.P., Howells, M.F., Bevins, R.E., Roach, R.A., and Dunkley, P.N., 1984, The Ordovician marginal basin of Wales, *in* Kokelaar, B.P., and Howells, M.F., eds., Marginal Basin Geology: Volcanic and Associated Sedimentary and Tectonic processes in Modern and Ancient Marginal Basins: Geological Society, London, Special Publication 16, p. 245–269, https://doi.org/10.1144/GSL.SP.1984.016.01.19.
Kunk, M.J., and Sutter, J.F., 1984, $^{40}Ar/^{39}Ar$ age spectrum dating of biotite from Middle Ordovician bentonites, eastern North America, *in* Bruton, D.I., ed. Aspects of the Ordovician System: Palaeontological Contributions from the University of Oslo, v. 295, p. 11–22.
Le Bas, M.J., 1972, Caledonian igneous rocks beneath central and eastern England: Proceedings of the Yorkshire Geological Society, v. 39, p. 71–86, https://doi.org/10.1144/pygs.39.1.71.
Leat, P.T., Jackson, S.E., Thorpe, R.S. and Stillman, C.J. 1986. Geochemistry of bimodal basalt-subalkaline/peralkaline rhyolite provinces within the southern British Caledonides. Journal of the Geological Society v. 143, p. 259-273.

© 2026 United Kingdom Research and Innovation.

Lee, M.K., Pharaoh, T.C., Williamson, J.P., Green, C.A., and De Vos, W., 1993, Evidence on the deep structure of the Anglo-Brabant Massif from gravity and magnetic data: Geological Magazine, v. 130, p. 575–582, https://doi.org/10.1017/S0016756800020872.

Linnemann, U., Herbosch, A., Liégeois, J.-P., Pin, C., Gärtner, A., and Hofmann, M., 2012, The Cambrian to Devonian odyssey of the Brabant Massif within Avalonia: A review with new zircon ages, geochemistry, Sm–Nd isotopes, stratigraphy and palaeogeography: Earth-Science Reviews, v. 112, p. 126–154, https://doi.org/10.1016/j.earscirev.2012.02.007.

Lipman, P.W., 1999, Calderas, *in* Sigurdsson, H., ed., Encyclopedia of Volcanoes: New York, Academic Press, p. 643–662.

Lusty, P.A.J., Lacinska, A.M., Millar, I.L., Barrie, C.D., and Boyce, A.J., 2017, Volcanological and environmental controls on the Snowdon mineralization, North Wales, UK: A failed volcanogenic massive sulfide system in the Avalon Zone of the British Caledonides: Ore Geology Reviews, v. 89, p. 557–586, https://doi.org/10.1016/j.oregeorev.2017.06.031.

Mattinson, J.M., 2005, Zircon U-Pb chemical-abrasion ("CA-TIMS") method: Combined annealing and multi-step dissolution analysis for improved precision and accuracy of zircon ages: Chemical Geology, v. 220, p. 47–66, https://doi.org/10.1016/j.chemgeo.2005.03.011.

McConnell, B.J., Stillman, C.J., and Hertogen, J., 1991, An Ordovician basalt to peralkaline rhyolite fractionation series from Avoca, Ireland: Journal of the Geological Society, v. 148, p. 711–718, https://doi.org/10.1144/gsjgs.148.4.0711.

McKerrow, W.S., Dewey, J.F., and Scotese, C.R., 1991, The Ordovician and Silurian development of the Iapetus Ocean, *in* Basset, M.G., et al., eds., The Murchison Symposium: Palaeontological Association of London, Special Papers in Palaeontology, v. 44, p. 165–178.

McLean, N.M., Condon, D.J., Schoene, B., and Bowring, S.A., 2015, Evaluating uncertainties in the calibration of isotopic reference materials and multi-element isotopic tracers (EARTHTIME Tracer Calibration Part II): Geochimica et Cosmochimica Acta, v. 164, p. 481–501, https://doi.org/10.1016/j.gca.2015.02.040.

Metzger, J.G., Ramezani, J., Bowring, S.A., and Fike, D.A., 2021, New age constraints on the duration and origin of the Late Ordovician Guttenberg $\delta^{13}C_{carb}$ excursion from high precision U-Pb geochronology of K-bentonites: Geological Society of America Bulletin, v. 133, p. 580–590, https://doi.org/10.1130/B35688.1.

Millward, D., and Evans, J.A., 2003, U–Pb chronology and duration of late Ordovician magmatism in the English Lake District: Journal of the Geological Society, v. 160, p. 773–781, https://doi.org/10.1144/0016-764902-160.

Min, K., Refine, P.R., and Huff, W.D., 2001, $^{40}Ar/^{39}Ar$ dating of Ordovician K-bentonites in Laurentia and Baltoscandia: Earth and Planetary Science Letters, v. 185, p. 121–134, https://doi.org/10.1016/S0012-821X(00)00365-4.

Molyneux, S.G., Harper, D.A.T., Cooper, M.R., Hollis, S.P., Raine, R.J., Rushton, A.W.A., Smith, M.P., Stone, P., Williams, M., Woodcock, N.H., and Zalasiewicz, J.A., 2023, A synopsis of the Ordovician System in its birthplace–Britain and Ireland, *in* Harper, D.A.T., Lefebvre, B., Percival, I.G., and Servais, T., eds., A Global Synthesis of the Ordovician System: Part 1: Geological Society, London, Special Publication 532, p. 191–266, https://doi.org/10.1144/SP532-2022-235.

Nathwani, C.L., Loader, M.A., Wilkinson, J.J., Buret, Y., Sievwright, R.H., and Hollings, P., 2020, Multi-stage arc magma evolution recorded by apatite in volcanic rocks: Geology, v. 48, p. 323–327, https://doi.org/10.1130/G46998.1.

Noble, S.R., Tucker, R.D., and Pharaoh, T.C., 1993, Lower Palaeozoic and Precambrian igneous rocks from eastern England, and their bearing on late Ordovician closure of the Tornquist Sea: Constraints from U-Pb and Nd isotopes: Geological Magazine, v. 130, p. 835–846, https://doi.org/10.1017/S0016756800023190.

Oruche, N.E., Dix, G.R., and Kamo, S.L., 2018, Lithostratigraphy of the upper Turinian–lower Chatfieldian (Upper Ordovician) foreland succession, and a U–Pb ID–TIMS date for the Millbrig volcanic ash bed in the Ottawa Embayment: Canadian Journal of Earth Sciences, v. 55, p. 1079–1102, https://doi.org/10.1139/cjes-2018-0006.

Pashley, V., Thomas, C., and Tapster, S., 2021, Uranium-lead (U-Pb) dating of the Wensleydale Granite, Yorkshire Dales, UK: NERC EDS National Geoscience Data Centre, Dataset, https://doi.org/10.5285/cf65a5b9-5d0e-4f23-90af-e98089b983c0.

Pearce, J.A., 1976, Statistical analysis of major element patterns in basalts: Journal of Petrology, v. 17, p. 15–43, https://doi.org/10.1093/petrology/17.1.15.

Pearce, J.A., 1983, Role of the subcontinental lithosphere in magma genesis at active continental margins, *in* Hawkesworth, C.J., and Norry, M.J., eds., Continental Basalts and Mantle Xenoliths: Leicester, UK, Shiva Publishing, p. 230–249.

Pearce, J.A., Harris, B.W., and Tindle, A.G., 1984, Trace element discrimination diagrams for the tectonic interpretation of granitic rocks: Journal of Petrology, v. 25, p. 956–983, https://doi.org/10.1093/petrology/25.4.956.

Pharaoh, T.C., 1999, Palaeozoic terranes and their lithospheric boundaries within the Trans-European Suture Zone (TESZ): A review: Tectonophysics, v. 314, p. 17–41, https://doi.org/10.1016/S0040-1951(99)00235-8.

Pharaoh, T.C., Merriman, R.J., Evans, J.A., Brewer, T.S., Webb, P.C., and Smith, N.J.P., 1991, Early Palaeozoic arc-related magmatism in the concealed Caledonides of southern Britain: Annales Société Géologique Belgique, v. 114, p. 63–92.

Pharaoh, T.C., Brewer, T.S., and Webb, P.C., 1993, Subduction-related magmatism of late Ordovician age in eastern England: Geological Magazine, v. 130, p. 647–656, https://doi.org/10.1017/S0016756800020951.

Pharaoh, T.C., England, R., and Lee, M.K., 1995, The concealed Caledonide basement of Eastern England and the southern North Sea—A review: Studia Geophysica et Geodaetica, v. 39, p. 330–346, https://doi.org/10.1007/BF02295826.

Pharaoh, T.C., Allsop, J.M., Holliday, D.W., Merriman, R.J., Kimbell, G.S., Rundle, C.C., Brewer, T.S., Noble, S.R., and Evans, C.J., 1997, The Moorby Microgranite: A deformed high level intrusion of Ordovician age in the concealed Caledonian basement of Lincolnshire: Proceedings of the Yorkshire Geological Society, v. 51, p. 329–342, https://doi.org/10.1144/pygs.51.4.329.

Phillips, B.A., Kerr, A.C., and Bevins, R.E., 2016, A re-appraisal of the petrogenesis and tectonic setting of the Ordovician Fishguard Volcanic Group, SW Wales: Geological Magazine, v. 153, p. 410–425, https://doi.org/10.1017/S0016756815000461.

Pidgeon, R.T., and Aftalion, M., 1978, Cogenetic and inherited zircon U-Pb systems in Palaeozoic granites from Scotland and England, *in* Bowes, D.R., and Leake, B.E., eds., Crustal Evolution in Northwest Britain and Adjacent Regions: Liverpool, UK, Seal House Press, Geological Journal Special Issue, v. 10, p. 183–220.

Prowatke, S., and Klemme, S., 2006, Trace element partitioning between apatite and silicate melts: Geochimica et Cosmochimica Acta, v. 70, p. 4513–4527, https://doi.org/10.1016/j.gca.2006.06.162.

Rollinson, H.R., 1993, Using Geochemistry Data: Evaluation, Presentation, Interpretation: Essex, UK, Longman Scientific and Technical Ltd., 352 p.

© 2026 United Kingdom Research and Innovation.

Schofield, D.I., Evans, J.A., Millar, I.L., Wilby, P.R., and Aspden, J.A., 2008, New U-Pb and Rb-Sr constraints on pre-Acadian tectonism in North Wales: Journal of the Geological Society, v. 165, p. 891–894, https://doi.org/10.1144/0016-76492008-044.
Sell, B., Ainsaar, L., and Leslie, S., 2013, Precise timing of the Late Ordovician (Sandbian) super- eruptions and associated environmental, biological, and climatological events: Journal of the Geological Society, v. 170, p. 711–714, https://doi.org/10.1144/jgs2012-148.
Sell, B.K., 2011, Intense volcanism and Ordovician icehouse climate, *in* Gutiérrez-Marco, J.C., Rábano, J., and Garcia-Bellido, D., eds., Ordovician of the World: Madrid, Cuadernos del Museo Geominero, Instituto Geológica y Minero de España, v. 14, p. 527–536.
Sell, B.K., and Samson, S.D., 2011, Apatite phenocryst compositions demonstrate a miscorrelation between the Millbrig and Kinnekulle K-bentonites of North America and Scandinavia: Geology, v. 39, p. 303–306, https://doi.org/10.1130/G31425.1.
Smit, J., van Wees, J.-D., and Cloetingh, S., 2016, The Thor Suture Zone: From subduction to intraplate basin setting: Geology, v. 44, p. 707–710, https://doi.org/10.1130/G37958.1.
Sun, S.-s., and McDonough, W.F.M., 1989, Chemical and isotopic systematics of oceanic basalts: Implications for mantle composition and processes, *in* Saunders, A.D., and Norry, M.J., eds., Magmatism in the Ocean Basins: Geological Society, London, Special Publication 42, p. 313–345, https://doi.org/10.1144/GSL.SP.1989.042.01.19.
Svensen, H.H., Hammer, Ø., and Corfu, F., 2015, Astronomically forced cyclicity in the Upper Ordovician and U-Pb ages of interlayered tephra, Oslo Region: Palaeogeography, Palaeoclimatology, Palaeoecology, v. 418, p. 150–159, https://doi.org/10.1016/j.palaeo.2014.11.001.
Thirlwall, M.F., and Fitton, J.G., 1983, Sm-Nd garnet age for the Ordovician Borrowdale Volcanic Group, English Lake District: Journal of the Geological Society, v. 140, p. 511–518, https://doi.org/10.1144/gsjgs.140.3.0511.
Torsvik, T.H., and Cocks, L.R.M., 2016, Earth History and Palaeogeography: Cambridge, UK, Cambridge University Press, 317 p., https://doi.org/10.1017/9781316225523.
Torsvik, T.H., and Rehnström, E.F., 2003, The Tornquist Sea and Baltica-Avalonia docking: Tectonophysics, v. 362, p. 67–82, https://doi.org/10.1016/S0040-1951(02)00631-5.
Tucker, R.D., and McKerrow, W.S., 1995, Early Paleozoic chronology: A review in light of new U-Pb zircon ages from Newfoundland and Britain: Canadian Journal of Earth Sciences, v. 32, p. 368–379, https://doi.org/10.1139/e95-032.
van Staal, C.R., and Barr, S., 2012, Lithospheric architecture and tectonic evolution of the Canadian Appalachians and associated Atlantic margin, *in* Clowes, R., Percival, J., and Cook, E., eds., Tectonic Styles in Canada: The LITHOPROBE Perspective: Geological Association of Canada Special Paper 49, p. 41–95.
Verniers, J.A., Pharaoh, T.C., André, L., Debacker, T.N., De Vos, W., Everaerts, M., Herbosch, A., Samuelsson, J., Sintubin, M., and Vecoli, M., 2002, The Cambrian to mid-Devonian basin development and deformation history of Eastern Avalonia, east of the Midlands Microcraton: New data and a review, *in* Winchester, J.A., Pharaoh, T.C., and Verniers, J., eds., Palaeozoic Amalgamation of Central Europe: Geological Society, London, Special Publication 201, p. 47–93, https://doi.org/10.1144/GSL.SP.2002.201.01.04.
Waldron, J.W.F., DuFrane, S.A., Schofield, D.I., and Barr, S.M., 2025, Is Britain divided by an Acadian suture?: Geology, v. 53, p. 847–852, https://doi.org/10.1130/G53431.1.
Webb, P.C., and Brown, G.C., 1989, Geochemistry of igneous rocks, *in* Plant, J.A., and Jones, D.G., eds., Metallogenic Models and Exploration Criteria for Buried Carbonate-Hosted Ore Deposits—A Multidisciplinary Study in Eastern England: Keyworth, Nottingham, UK, British Geological Survey, and London, The Institution of Mining and Metallurgy, p. 95–122.
Whalen, J.B., and Hildebrand, R.S., 2019, Trace element discrimination of arc, slab failure, and A-type granitic rocks: Lithos, v. 348, p. 348–367, https://doi.org/10.1016/j.lithos.2019.105179.
Whalen, J.B., Currie, K.L., and Chappell, B.W., 1987, A-type granites: Geochemical characteristics, discrimination and petrogenesis: Contributions to Mineralogy and Petrology, v. 95, p. 407–419, https://doi.org/10.1007/BF00402202.
Williamson, J.P., Pharaoh, T.C., Banka, D., Thybo, H., Laigle, M., and Lee, M.K., 2002, Potential field modelling of the Baltica-Avalonia (Thor-Tornquist) suture beneath the southern North Sea: Tectonophysics, v. 360, p. 47–60, https://doi.org/10.1016/S0040-1951(02)00346-3.
Wilson, C.J.N., Houghton, B.F., McWilliams, M.O., Lanphere, M.A., Weaver, S.D., and Briggs, R.M., 1995, Volcanic and structural evolution of Taupo Volcanic Zone, New Zealand: A review: Journal of Volcanology and Geothermal Research, v. 68, p. 1–28, https://doi.org/10.1016/0377-0273(95)00006-G.
Winchester, J.A., and the PACE TMR Network Team, 2002, Palaeozoic amalgamation of Central Europe: New results from recent geological and geophysical investigations: Tectonophysics, v. 360, p. 5–21, https://doi.org/10.1016/S0040-1951(02)00344-X.

SCIENCE EDITOR: MIHAI DUCEA
ASSOCIATE EDITOR: JEAN BÉDARD

MANUSCRIPT RECEIVED 11 SEPTEMBER 2025
REVISED MANUSCRIPT RECEIVED 29 JANUARY 2026
MANUSCRIPT ACCEPTED 6 APRIL 2026

© 2026 UNITED KINGDOM RESEARCH AND INNOVATION.